25

Time–Frequency Signal Processing for Wireless Communications

Boualem Boashash
Queensland University of Technology

A. Belouchrani
Ecole Nationale Polytechnique

Karim Abed-Meraim
Telecom

Nguyen Linh-Trung
Queensland University of Technology

Abstract

This chapter is intended to relate recent advances in the field of time–frequency signal processing (TFSP) to the need for further capacity of wireless communications systems. It first presents, in a brief and heuristic approach, the fundamentals of TFSP. It then describes the TFSP-based methodologies that are used in wireless communications with special emphasis on spread-spectrum techniques and time–frequency array processing. Topics discussed include channel modeling and identification, estimation of scattering function, interference mitigation, direction of arrival estimation, time–frequency MUSIC, and time–frequency source separation. Finally, other emerging applications of TFSP to wireless communications are discussed.

0-8493-1657-X/$0.00+$1.50

25.1 Introduction

Wireless communications is growing at an explosive rate, stimulated by a host of important emerging applications ranging from third-generation mobile telephony, wireless personal communications, and wireless subscriber loops, to radio and infrared indoor communications, nomadic computing, and wireless tactical military communications. Signal processing has played a key role in providing solutions to key problems encountered in communications in general, and in wireless communications in particular [1]. An important branch of signal processing called time–frequency signal processing (TFSP) has emerged over the past decades [2, 3]. It provides effective tools for analyzing nonstationary signals where the frequency content of signals varies in time, as well as for analyzing linear time-varying systems. The purpose of this chapter is to review the methodologies of TFSP applied to wireless communications.

Fundamental issues in wireless communications include the problems of *interference mitigation in CDMA* (code-division multiple access) or multicarrier CDMA (MC-CDMA), and *array processing* for source localization and signal separation.

Along with channel fading, there exist many types (inherent and noninherent) of interference causing degradation in the system performance, hence reducing the system capacity. In addition to the high capacity resulting from the smart way of providing multiple access, CDMA has shown advantages over many other multiple-access schemes in terms of reducing the effects of interference and multipathfading [13]. CDMA has in fact been selected to be the basic building block for third-generation wireless communications (wideband CDMA) [14], and the promising candidate for the fourth generation (generalized multicarrier CDMA) [15]. However, to achieve the best system performance, it is still very crucial to minimize the effects of various types of interference in CDMA systems, namely, narrowband interference (NBI) [16], multiple-access interference (MAI) [17], and, for high-data-rate applications, intersymbol interference (ISI).

When multiple sensors are available at the receiver side, array processing techniques can be used to achieve source (mobile) localization or source separation. Source localization is of great importance in radar/sonar applications but also in wireless mobile communications. Mobile localization can add a number of important services to the capabilities of cellular systems, including help for mobile navigation, emergency services (also known as E-911 problem), location-sensitive billing, fraud protection, and person/asset tracking [74].

The problem of source separation or blind source separation (BSS) arises when considering MIMO (multi-input multi-output) systems where BSS techniques are used to solve the MAI problem and to extract the desired information for each user.

On the other hand, received signals are generally nonstationary due to source signal's nonstationaries or to the time-varying nature of propagation channels. Indeed, the wireless communication environment exhibits a multipath propagation phenomenon with Doppler effect, where the received signal is not only affected by additive Gaussian noise but also by a sum of attenuated, delayed, and Doppler-shifted versions of the transmitted signal [5, 6]. As a result, the received signals are affected in strength and shape, depending on different environments (indoor, outdoor, urban, suburban), speed of mobile agent or surrounding movements, and signaling (bandwidth, data rate, modulation, and carrier frequency). The transmitted signals undergo serious fading through the propagation channel. Especially in wideband wireless communications, the underlying channel exhibits a random linear time-varying (LTV) characteristic and is most commonly assumed to be a wide-sense stationary uncorrelated scattering (WSSUS) process [9–12].

All these wireless communication problems involve a time-varying context, and therefore the use of TFSP techniques should lead to improvements in system performance.

The focus of this chapter is to review such TFSP techniques and clarify the methodologies of TFSP that are most relevant for use in wireless communications. The structure of the chapter is as follows: Section 25.2 briefly introduces the basics of TFSP in order to provide a better insight for the review in the parts that follow. Section 25.3 reviews some applications of TFSP techniques in spread-spectrum communication systems. Section 25.4 describes array signal processing techniques using time–frequency distributions (TFDs). And finally, Section 25.5 briefly reviews some other issues encountered in wireless communications where the TFSP techniques play a central role.

25.2 Time–Frequency Signal Processing Tools

TFSP is a relatively new field comprised of signal processing methods, techniques, and algorithms in which the two natural variables time, t, and frequency, f, are used *concurrently* in contrast with the traditional signal processing methods where time and frequency variables are used exclusively and independently. The observation of natural phenomena indicates that these two variables, t and f, are usually simultaneously present in signals (e.g., natural frequency-modulated (FM) signals such as the song of some birds). Such signals are called nonstationary because their spectral characteristics vary with time [21]. TFSP is designed to deal effectively with such signals by allowing their detailed and precise analysis and processing. It also enables the design and synthesis of signals and systems with specific time and frequency characteristics, suitable to applications such as wireless communications.

25.2.1 Limitations of Traditional Signal Representations

The spectrum of a signal (deterministic or random) gives no indication as to how the frequency content of a signal changes with time, information that is important when one deals with a large class of nonstationary signals such as FM signals. This frequency variation often contains critical information about the signal and the process inherent to real-life applications.[1]

The limitation of 'classical' spectral representations is better illustrated by the fact that we can find totally different signals (related to different physical phenomena), $s_a(t)$ and $s_b(t)$, which yet have the same spectra (that is, magnitude spectra) — see Figure 25.2. Representing signals in a way that is useful for precise characterization and identification serves as a part of the motivation for devising a more sophisticated and practical nonstationary signal analysis tool, which preserves all the information of the signal, and therefore discriminates signals in a better way, using one single complete representation instead of attempting to interpret magnitude and phase spectra separately.

25.2.2 Joint Time–Frequency Representations

25.2.2.1 Finding Hidden Information Using Time–Frequency Representations

Revealing the time and frequency dependence of a signal, such as a linear FM (LFM) signal, is achieved by using a joint time–frequency representation such as the one shown in Figure 25.1.[2]

In this representation, the start and stop time instants are clearly identifiable, as is the time variation of the frequency content of the signal described by the linear pattern of peaks. (This information cannot be retrieved solely from either the instantaneous power $|s(t)|^2$ or the spectrum representations $|S(f)|^2$. It is lost when the Fourier transform is squared in modulus and the phase of the spectrum is thereby discarded.) The spectrum phase contains the actual information about the internal organization of the signal, such as details of time instants at which the signal has energy above or below a particular threshold, and the order of appearance in time of the different frequencies present in the signal. The difficulty of interpreting and analyzing a phase spectrum makes the concept of a joint time–frequency signal representation attractive.

Example 25.1

Figure 25.2 illustrates another example of two slightly different signals with the same spectrum that could not be properly analyzed without a joint time–frequency representation. Both signals contain three LFMs whose start and stop times are different. The differences are not shown easily in the t or f domain, but

[1] This information is encoded in the phase spectrum. However, it generally is not used, as it is difficult to interpret and analyze a phase spectrum.

[2] In this example the Wigner–Ville distribution (WVD) is used, as it provides the optimal joint time–frequency distribution (TFD) for an LFM signal [21].

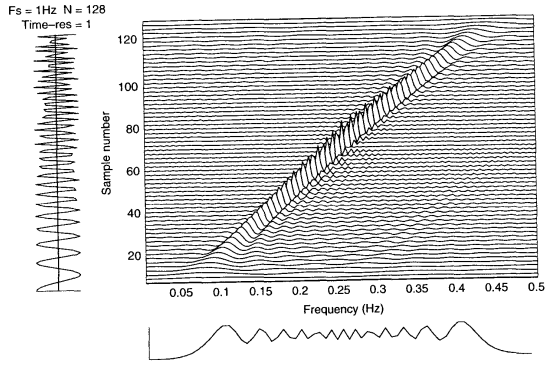

FIGURE 25.1 Time–frequency representation of a linear FM signal: the signal's time domain representation appears on the left, and its spectrum on the bottom.

appear clearly in the $t - f$ representation, which allows precise and simultaneous measurements of actual frequencies and their epochs. The B distribution (BD) [18] is used to represent two signals in the $t - f$ domain.

Figure 25.2 also indicates another significant reason to use joint time–frequency representations of signals: it reveals whether the signal is monocomponent or multicomponent, a fact that cannot be revealed by conventional spectral analysis, especially when individual components are also time varying, such as the six chirps in the figure.

25.2.2.2 What Is a Time–Frequency Representation?

TFSP is a natural extension of both time domain and frequency domain processing that involves representing signals in a complete space that can display all the signal information in a more accessible way [2]. Such a representation is intended to provide a *distribution* of signal energy, $E(t, f)$, vs. both time and frequency simultaneously. For this reason, the representation is commonly called a TFD.

A concept intimately related to joint time–frequency representation is that of instantaneous frequency (IF) and time delay (TD). The IF corresponds to the frequency of a sine wave that locally (at a given time) fits the signal under analysis. The TD is a measure of the order of arrival of the frequencies.

The TFD is expected to visually exhibit in the $t - f$ domain the time–frequency law of each signal component, thereby making the estimation of the IF, $f_i(t)$, and TD, $\tau_d(f)$, easier, and could also provide additional information about relative component amplitudes, and the spectral spread of the component around the IF (the spread is known as the instantaneous bandwidth, $B_i(t)$).

The TFD is often expected to satisfy a certain number of properties that are intuitively desirable for a practical analysis. Let us denote by $\rho_z(t, f)$ a TFD that is a time–frequency representation of signal $z(t)$. $\rho_z(t, f)$ is expected to satisfy the following properties:

- P1a: The TFD should be real and its integration over the whole time–frequency domain results in the total signal energy E_z:

$$\int_{-\infty}^{\infty}\int_{-\infty}^{\infty} \rho_z(t, f)dt\,df = E_z \tag{25.1}$$

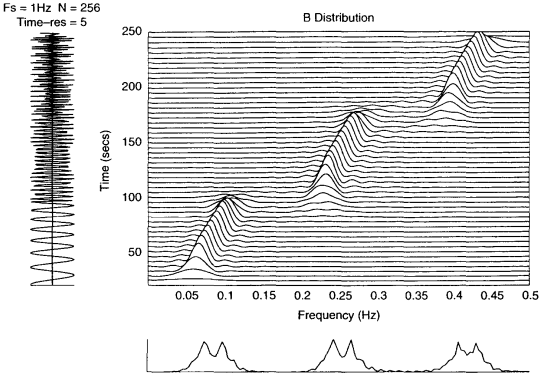

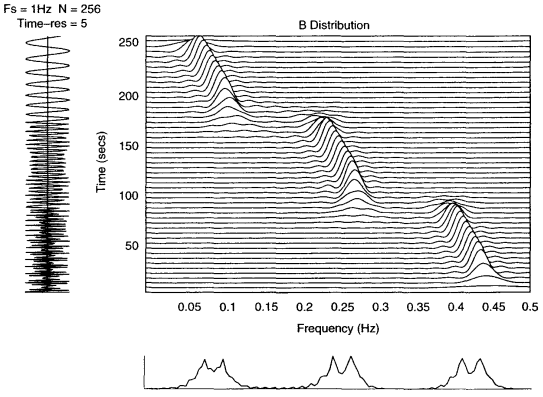

FIGURE 25.2 Time–frequency representation of two different three-component signals (using B distribution).

- P1b: It would also be desirable that the energy in a certain region R in the $t - f$ plane, E_{z_R}, be expressible as in Equation 25.1, but with limits of integration restricted to the boundaries $(\Delta t, \Delta f)$ of the region R:

$$E_{z_R} = \int_{\Delta t}\int_{\Delta f} \rho_z(t, f)dt\,df \tag{25.2}$$

which is a portion of signal energy in the band Δf and time interval Δt.

- P2: The peak of the TFD and the first moment of the time–frequency representation with respect to frequency should be equal to the IF of a monocomponent signal:

$$f_i(t) = \frac{\int_{-\infty}^{\infty} f\rho_z(t,f)df}{\int_{-\infty}^{\infty} \rho_z(t,f)df} \tag{25.3}$$

- P3: For multicomponent signals, the peaks of the TFD should exhibit the various IF laws of individual components without the nuisance of ghost terms or interferences.

There are also some other properties, which were earlier seen as strictly needed, but were found later not to be, as detailed in Chapter 3 of [3]. For example, early researchers indicated that a TFD should reduce to the spectrum and instantaneous power by integrating over one of the variables, so that

$$\int_{-\infty}^{\infty} \rho_z(t,f)dt = |S_z(f)|^2 \tag{25.4}$$

$$\int_{-\infty}^{\infty} \rho_z(t,f)df = |z(t)|^2 \tag{25.5}$$

These two conditions are often called marginal conditions. However, it was shown that some high resolution TFDs could be generated that did not meet the marginals [3].

Another property that was originally seen as desirable is positivity, but it was shown to be incompatible with P2 [21], which is more important in practice.

A number of questions arise from the above: Can we design a TFD that meets the specifications listed above? If yes, how can we do it? What are the significant signal characteristics and parameters that will impact the construction of a joint time–frequency representation? How do these relate to the TFD? How do we obtain them from the time–frequency representation? The answers to these questions are important in formulating efficient time–frequency methodologies specifically adapted for applications such as wireless communications and will be briefly discussed in the next sections. More details can be found in [3, Chapters 2 and 3] and [19].

25.2.2.2.1 Physical Interpretation of TFDs

Most TFDs used for a practical time–frequency signal analysis are not necessarily positive-definite, so they do not represent an instantaneous energy spectral density at time t and frequency f. For example, the Page distribution describes the rate of change of the spectrum and is defined as the time derivative of the running spectrum (spectrum of the signal from $-\infty$ to time t), and hence can take both positive and negative values:

$$\rho_{z_P}(t,f) = \frac{\partial}{\partial t}\left|\int_{-\infty}^{t} z(u)e^{-j2\pi fu}du\right|^2$$

To relate $\rho_z(t,f)$ to the physical quantities used in practical experimentation, we can interpret $\rho_z(t,f)$ as a measure of energy flow through the spectral window $(f-\Delta f/2, f+\Delta f/2)$ during the time interval $(t-\Delta t/2, t+\Delta t/2)$. The signal energy localized in this time–frequency domain, $(\Delta t, \Delta f)$, is then given by

$$E_{\Delta t,\Delta f} = \int_{t-\Delta t/2}^{t+\Delta t/2}\int_{f-\Delta f/2}^{f+\Delta f/2} \rho_z(t,f)dt\,df \tag{25.6}$$

The larger the window, the more likely $E_{\Delta t,\Delta f}$ will correspond to a true measure of physical energy. The window should be chosen large enough so that $\Delta t\Delta f$ satisfies Heisenberg's uncertainty relation [2]: $\Delta t\Delta f \geq 1/(4\pi)$.

25.2.2.2.2 Instantaneous Frequency and Group Delay

The IF, $f_i(t)$, of a monocomponent signal is a measure of the localization in time of the individual frequency components of the signal [2].

The IF, $f_i(t)$, of a monocomponent *analytic* signal[3] $z(t) = a(t)e^{j\phi(t)}$ is given by

$$f_i(t) = \frac{1}{2\pi}\frac{d\phi(t)}{dt} \tag{25.7}$$

The IF of a monocomponent *real* signal $s(t) = a(t)\cos\phi(t)$ is defined as the IF of the analytic signal $z(t)$ corresponding to $s(t)$. The expressions of the IF given above do not apply directly to multicomponent signals. For such signals, the expression of the IF needs to be applied to its individual components to have a meaningful physical interpretation.

The twin of the IF concept in the frequency domain is called the time delay, $\tau_d(f)$.

The TD of a monocomponent *analytical* signal $z(t)$ is defined as

$$\tau_d(f) = -\frac{1}{2\pi}\frac{d\theta(f)}{df} \tag{25.8}$$

where

$$\mathcal{F}\{z(t)\} = Z(f) = A(f)e^{j\theta(f)} \tag{25.9}$$

$\mathcal{F}\{\cdot\}$ stands for Fourier transform (FT). Equations 25.7 and 25.8 are similar except for the minus sign, in the same way that the FT and inverse FT (IFT) are similar except for a minus sign in the exponent of the basis function $e^{j2\pi ft}$.

The TD of a monocomponent *real* signal $s(t)$ is defined as the TD of the analytic signal $z(t)$ corresponding to $s(t)$.

The order of appearance of each time-varying frequency component is the TD. The global order of appearance of the frequencies is called the group delay (a mean value of individual TDs).

The IF and TD describe the internal organization of the signal. Neglecting this information would result in a lack of precision of the information characterizing the signal, as illustrated in [3, p. 7, Figure 1.1.2].

25.2.3 Quadratic Time–Frequency Distributions

25.2.3.1 Time-Varying Spectrum and the Wigner–Ville Distribution

To determine why time information appears to be lost when we take the power spectral distribution (PSD) and how it can be recovered, let us consider a complex random process $Z(t)$ with realizations $z(t,\epsilon)$, where ϵ represents the ensemble index identifying each realization. To improve clarity, we simply replace $z(t,\epsilon)$ by $z(t)$. (ϵ is implicit when we say that $z(t)$ is random.)

The autocorrelation function of $z(t)$ may be defined in symmetric form as

$$\begin{aligned} R_z(t,\tau) &= E\{z(t+\tau/2)z^*(t-\tau/2)\} \\ &= E\{K_z(t,\tau)\} \end{aligned} \tag{25.10}$$

where $K_z(t,\tau) = z(t+\tau/2)z^*(t-\tau/2)$ is the signal kernel and $E\{\cdot\}$ denotes the expected value operator.

The Wiener–Khintchine theorem states that for a stationary signal, the signal power spectral density equals the FT of its autocorrelation function.

[3] The analytic signal $z(t)$ associated with the real signal $x(t)$ is defined as

$$z(t) = x(t) + j\mathcal{H}\{x(t)\}$$

where $\mathcal{H}\{\ \}$ represents the Hilbert transform [21].

By extension to TD random signals, the time-varying PSD, $S_z(t,f)$, is defined as the FT of the time-varying autocorrelation function, $R_z(t,\tau)$, i.e.,

$$\begin{aligned} S_z(t,f) &= \underset{\tau\to f}{\mathcal{F}} \quad [R(t,\tau)] \\ &= \underset{\tau\to f}{\mathcal{F}} \quad E\{K_z(t,\tau)\} \qquad (25.11) \\ &= E\left\{\underset{\tau\to f}{\mathcal{F}} \quad [K_z(t,\tau)]\right\} \\ &= E\{W_z(t,f)\} \qquad (25.12) \end{aligned}$$

where the interchange of E and FT is made under the assumptions verified by the class of bounded amplitude finite-duration signals [3], and $W_z(t,f)$ is referred to as the Wigner–Ville distribution (WVD), expressed as

$$\begin{aligned} W_z(t,f) &= \underset{\tau\to f}{\mathcal{F}}[K_z(t,\tau)] \\ &= \underset{\tau\to f}{\mathcal{F}}[z(t+\tau/2)z^*(t-\tau/2)] \qquad (25.13) \end{aligned}$$

The problem of estimating the time-varying PSD of a random process $z(t)$ is thus one of averaging the WVD of the process over ϵ. If only one realization of the signal is available, assuming the signal is locally ergodic[4] over a window, an estimate of the time-varying PSD is obtained by smoothing the WVD over the window of local ergodicity [21].

25.2.3.2 Time-Varying Spectrum Estimates and Quadratic TFDs

If $z(t)$ is deterministic, from Equation 25.12, $S_z(t,f)$ reduces to $W_z(t,f)$, i.e.,

$$S_z(t,f) = E\{W_z(t,f)\} = W_z(t,f) \qquad (25.14)$$

- The signals we consider have a finite-duration T. This fact can be expressed by introducing a finite-duration time window $g_1(t)$, hence convolving $S_z(t,f)$ in the frequency direction with $G_1(f) = \mathcal{F}[g_1(t)]$.[5]
- In practice, signals also have finite bandwidth restrictions. This introduces a frequency window $G_2(f)$, convolving $S_z(t,f)$ in the time direction with $g_2(t)$ (the IFT of $G_2(f)$: $g_2(t) = \mathcal{F}^{-1}\{G_2(f)\}$).
- By combining the separable windowing effects of $g_1(t)$ in time and $G_2(f)$ in frequency, the above leads to

$$\hat{S}_z(t,f) = W_z(t,f) \star_f G_1(f) \star_t g_2(t)$$

  where $\star_t$ and $\star_f$ indicate convolution in time and frequency, respectively, and $G_1(f)$ and $g_2(t)$ are even functions (such as those traditionally used in spectral analysis and digital filter design).
- The above formulation was introduced step by step to illustrate the two-dimensional convolution that is inherent to signals that have nearly finite duration and bandwidth (most real-life signals). This formulation is a special case where the two-dimensional windowing in t and f is separable.
- In general, we need to introduce an even function[6] $\gamma(t,f)$ that may or may not be separable and that reflects the overall duration–bandwidth limitation in both time and frequency. This leads to

[4] In essence, a random process is ergodic if its ensemble averages equal its time averages.

[5] For simplicity, $\mathcal{F}$ instead of $\underset{t\to f}{\mathcal{F}}$ where no ambiguity occurs.

[6] A real and even signal has a real and even FT.

the following general formulation of time–frequency representations:

$$\hat{S}_z(t,f) \equiv \rho_z(t,f) = W_z(t,f) \star_t \star_f \gamma(t,f) \qquad (25.15)$$

where the double star indicates convolution in both time and frequency, $\hat{S}_z(t,f)$ is the time-varying estimate of the PSD, $W_z(t,f)$ is the WVD, and $\gamma(t,f)$ is an even function which defines the TFD and its properties.

By expanding $W_z(t,f)$ and the double convolution in Equation 25.15, we obtain the following general quadratic form:

$$\rho_z(t,f) = \int_{-\infty}^{\infty}\int_{-\infty}^{\infty}\int_{-\infty}^{\infty} e^{j2\pi\nu(u-t)} g(\nu,\tau) z\left(u+\frac{\tau}{2}\right) z^*\left(u-\frac{\tau}{2}\right) e^{-j2\pi f\tau}\, d\nu\, du\, d\tau \qquad (25.16)$$

where $g(\nu,\tau)$ is the two-dimensional FT of $\gamma(t,f)$. The function $g(\nu,\tau)$ determines how the signal energy is distributed in time and frequency. It is analogous to the windows used in the classical spectral analysis. By appropriately choosing $g(\nu,\tau)$, we can obtain most of the popular time–frequency representations of signals [21].

25.2.3.3 Time, Lag, Frequency, and Doppler Domains and the Ambiguity Function

We have defined in Equation 25.13 the WVD of signal $z(t)$ as the FT of the signal kernel $K_z(t,\tau)$, i.e.,

$$W_z(t,f) = \underset{\tau\to f}{\mathcal{F}}\{K_z(t,\tau)\}$$

The time-average autocorrelation function of a deterministic signal $z(t)$ may be defined as the inverse FT of its energy spectrum $|Z(f)|^2$, i.e.,

$$R_z(\tau) = \mathcal{F}^{-1}\{|Z(f)|^2\}$$

$R_z(\tau) = \int_{-\infty}^{\infty} z(t+\frac{\tau}{2})z^*(t-\frac{\tau}{2})dt$ is a measure of the similarity between the signal and its time-delayed copies and is obtained by taking the integral over time of the signal kernel $K_z(t,\tau)$.

Another quantity that makes use of $K_z(t,\tau)$ is the symmetric ambiguity function (AF) [21]:

$$\begin{aligned} A_z(\nu,\tau) &= \int_{-\infty}^{\infty} K_z(t,\tau) e^{-j2\pi\nu t} dt \\ &= \int_{-\infty}^{\infty} z\left(t+\frac{\tau}{2}\right) z^*\left(t-\frac{\tau}{2}\right) e^{-j2\pi\nu t} dt \qquad (25.17) \end{aligned}$$

Equation 25.17 represents the basic radar equation obtained by correlating a signal with the same signal delayed in time by lag τ and shifted in frequency by Doppler ν. The ambiguity domain also represents directly the effects of multipath-delay spread and Doppler-shift spread, which characterize the time-varying nature of wireless communication channels. It can therefore be used to analyze the behavior of signals in wireless communications and control the effects of spreading.

The key point here is the role played by $K_z(t,\tau)$ in the formulation of many important signal processing concepts. We showed that time–frequency, time-lag, and Doppler-lag representations (as well as Doppler-frequency representations) can be obtained from the signal kernel by means of FT and IFT. This is illustrated in Figure 25.3.

Figure 25.3 indicates that the two-dimensional FT of the WVD of signal $z(t)$ equals the symmetric AF $A_z(\nu,\tau)$ of $z(t)$ (as indicated by the two vertical arrows):

$$W_z(t,f) \overset{t}{\underset{f}{\rightleftharpoons}} \overset{\nu}{\underset{\tau}{}} A_z(\nu,\tau)$$

This property is important in TFSP. It indicates that the twin of the time–frequency domain is the lag-Doppler domain (also called the ambiguity domain). The (t,f) domain represents the signal as a function of actual time and actual frequency, while the (ν,τ) domain represents the signal as a function

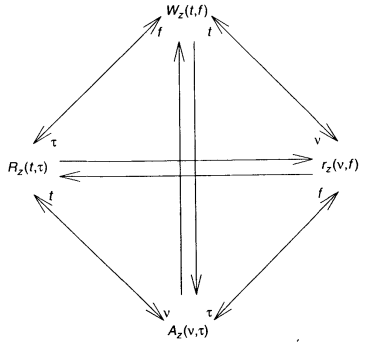

FIGURE 25.3 Various representations that can be obtained from the signal kernel $K_z(t,\tau)$.

of time shifts and frequency shifts. Hence, a double convolution in (t, f) results (by two-dimensional FT) in a multiplication in the ambiguity domain. This leads to the interpretation of TFD design, defined by Equation 25.15, as a two-dimensional filtering procedure in the ambiguity domain. Equation 25.16 can therefore be rewritten as the two-dimensional FT of the symmetric AF $A_z(\nu,\tau)$ filtered by the kernel filter $g(\nu,\tau)$:

$$\rho_z(t,f) \overset{t}{\underset{f}{\rightleftharpoons}} g(\nu,\tau) A_z(\nu,\tau) \tag{25.18}$$

Choosing the kernel filter $g(\nu,\tau)$ most relevant to an application results in a specific TFD. For an all-pass filter, $g(\nu,\tau) = 1$, $\rho_z(t,f)$ reduces to the WVD, which may be expressed as

$$W_z(t,f) = \underset{\tau\to f}{\mathcal{F}}[K_z(t,\tau)] = \underset{\tau\to f}{\mathcal{F}}[z(t+\tau/2)z^*(t-\tau/2)] \tag{25.19}$$

For $g(\nu,\tau)$ chosen to be the AF of the time analysis window $h(t)$, it reduces to the spectrogram, which may be expressed as

$$\rho_{spec}(t,f) = |\mathcal{S}(t,f)|^2 = \left|\int_{-\infty}^{\infty} s(\tau)h(\tau-t)e^{-j2\pi f\tau}d\tau\right|^2 \tag{25.20}$$

where $\mathcal{S}(t,f)$ is the short-time Fourier transform (STFT).

Using a symmetrical rectangular window of width T, $h(t) = rect(t/T)$, the above equation reduces to

$$\rho_{spec}(t,f) = \left|\int_{t-T/2}^{t+T/2} s(\tau)e^{-j2\pi f\tau}d\tau\right|^2 \tag{25.21}$$

This is obtained from the general form (Equation 25.20) by selecting the kernel filter to be

$$g(\nu,\tau) = rect(\tau/2T)\frac{\sin\pi(T-|\tau|)\nu}{\pi\nu} \tag{25.22}$$

The next section presents some important considerations relevant to the selection of suitable kernel filters.

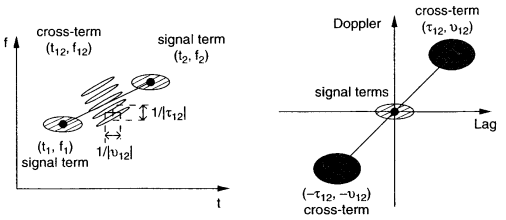

FIGURE 25.4 Position of signal terms and cross-terms in both time–frequency and Doppler-lag domains.

25.2.3.4 Quadratic TFDs, Multicomponent Signals, Cross-Terms Reduction, and Criteria for the Design of Quadratic TFDs

Equation 25.16 defines TFDs that are quadratic (or bilinear) in the signal $z(t)$. This implies that if the signal $z(t)$ includes two components $z_1(t)$ and $z_2(t)$, then its quadratic formulation will include not only these two components but also additional components corresponding to their cross-product $z_1(t)z_2(t)$. These additional components are often called cross-terms and are considered "artifacts" or "ghosts" appearing unexpectedly in the $t-f$ representation (see Figure 25.4). A similar effect occurs when we take the spectrum of $z_1(t) + z_2(t)$ and obtain cross-spectral components that are zero only when $z_1(t)$ and $z_2(t)$ do not overlap in frequency (see Figure 25.5) [3].

Thus, the introduction of either noise or some other deterministic components introduces significant cross-terms into the representation. In some applications these cross-terms may be useful as they provide

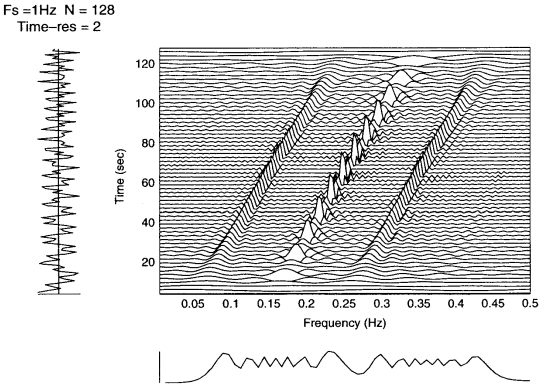

FIGURE 25.5 WVD of a signal composed of two linear frequency modulations exhibiting large positive and negative amplitudes commonly known as cross-terms.

additional features that can be used for signal identification and recognition. However, in most cases, they are considered undesirable interference terms that distort the reading of the representation, and we want to design TFDs that suppress them best.

25.2.3.4.1 Reduced Interference Distributions

Several TFDs have been designed for this purpose. One of the best known is the Gaussian distribution (also called Choi–Williams distribution (CWD)) whose kernel filter $g(\nu, \tau)$ is a two-dimensional Gaussian function centered around the origin in the ambiguity plane and whose spread is controlled by a parameter σ (hence controlling the amount of cross-terms reduction and autoterms resolution). Another recently introduced TFD is the BD [18], whose time-lag kernel filter is defined as

$$G(t,\tau) = \left(\frac{|\tau|}{\cosh^2(t)}\right)^{\beta} \tag{25.23}$$

where $0 < \beta \leq 1$ is an application-dependent parameter that controls the sharpness of the cutoff of the two-dimensional filter in the ambiguity domain, resulting in a trade-off between time–frequency resolution and cross-terms elimination. Cross-terms can be reduced by making β small. An improved version, the modified BD (MBD) was defined in [3, Article 5.7].

Resolution performance of various TFDs, when used to represent multicomponent signals, can be measured using an objective measure that takes into account the key attributes of TFDs (such as the amplitudes of autoterms and cross-terms, autoterms' bandwidth and sidelobes' amplitudes) [18].

25.2.3.4.2 Comparison of Quadratic TFDs

Using the above mentioned-objective measure, the BD and its modified version (MBD) [3] were found to be among the closest to the ideal distribution; the BD is essentially cross-term-free and has high resolution in the time–frequency plane (see Figure 25.6). This TFD outperforms the spectrogram and other existing reduced interference distributions in the analysis of multicomponent signals, and is practically 'equivalent' to the WVD in the analysis and estimation of a monocomponent linear FM signal (see [3, 18, 19] for more details). For this reason, we will often refer to it in this chapter in conjunction with other methods like the WVD, spectrogram, and Gaussian distribution.

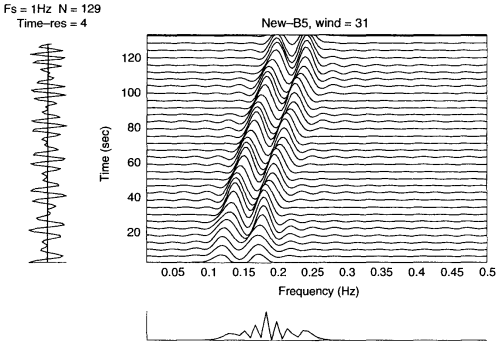

FIGURE 25.6 The B distribution of two closely spaced linear FM signals.

25.2.3.5 Time–Frequency Signal Synthesis

Whereby TF signal analysis algorithms are used to analyze the time-varying frequency behavior of signals, TF signal synthesis algorithms are used to synthesize (or estimate) signals whose TFDs exhibit some given time-varying frequency characteristics. This problem can be formulated as follows: if $z(t)$ is a signal of interest with $\rho_z(t, f)$ being its TFD in the general quadratic class, the synthesis problem is to find the analytic signal $\hat{z}(t)$ whose TFD, $\rho_{\hat{z}}(t, f)$, best approximates $\rho_z(t, f)$ according to some defined criteria. One of the earliest algorithms for TF signal synthesis was based on the WVD in [20]. Some improvements and extensions were made in [21–25]. Several other methods can be found in [3].

The basis of the WVD-based algorithm is the inversion property of the WVD [2]:

$$z(t) = \frac{1}{z^*(0)} \int W_z(t/2, f)\, e^{j2\pi f t}\, df \tag{25.24}$$

implying that the signal may be reconstructed to within a complex exponential constant $e^{j\alpha} = z^*(0)/|z(0)|$ given $|z(0)| \neq 0$.

25.2.3.6 Other Properties

Another important property of quadratic TFDs is their compatibility with filtering. This property expresses the fact that if a signal $y(t)$ is the convolution of $x(t)$ and $h(t)$ (i.e., $y(t)$ is the output of a linear time-invariant filter with impulse response $h(t)$ whose input is $x(t)$), the TFD of $y(t)$ is the time convolution between the TFD of $x(t)$ and the WVD of $h(t)$. Mathematically, if

$$y(t) = x(t) * h(t)$$

then

$$\rho_y(t, f) = \rho_x(t, f) \underset{t}{*} W_h(t, f) \tag{25.25}$$

The properties of quadratic TFDs discussed above are shown in the next sections to be relevant to providing efficient solutions to several problems arising in wireless communications, allowing for improved system performance. For space reasons, techniques such as IF estimation [53] and cross-WVD (XWVD) [3, Chapter 3] are not discussed here. Interested readers can refer to the references provided.

25.3 Spread-Spectrum Communications Systems Using TFSP

Spread-spectrum communications use signals whose bandwidth is much wider than the information bandwidth. This is achieved by the direct-sequence (DS) technique in which the transmitted signal is spread over a wide bandwidth by means of a code independent of the data. The availability of this code at the receiver enables the despreading and recovery of data, while spreading and mitigating the interference (see Figure 25.7). Spread-spectrum techniques offer a number of important advantages, such as code-division multiple access, low probability of intercept, communications over multipath propagation channels, and resistance to intentional jamming. The processing gain of a DS spread-spectrum system, generally defined as the ratio between the transmission and the data bandwidths, provides the system with a high degree of interference mitigation. However, in some cases, the interference might be much stronger than the useful signal, e.g., when the useful signal is affected by fading and the gain due to the coding might be insufficient to decode the useful signal reliably. Therefore, time–frequency (TF) signal processing techniques have been used in conjunction with the signal spreading to augment the processing gain, permitting greater interference protection without an increase in bandwidth. In this section, we review some of these TF signal processing techniques for channel identification and interference mitigation.

25.3.1 Channel Modeling and Identification

In this section we show how time–frequency representations of a linear time-varying propagation channel can be exploited for channel estimation either by direct use of the observation signal TFD as in [7], by

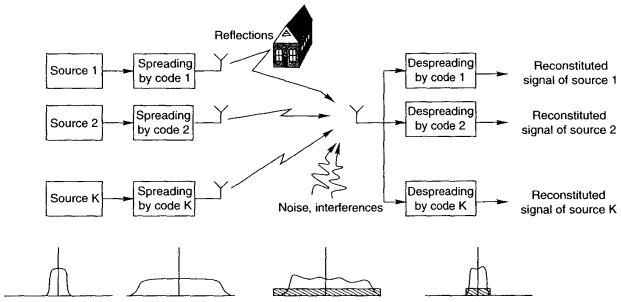

FIGURE 25.7 DS-CDMA communications system.

time–frequency polynomial modeling as in [8], or by using time–frequency canonical channel modeling, which we describe in Sections 25.3.1.1 and 25.3.1.2 since it is the most commonly used LTV channel estimation method.

25.3.1.1 Wireless Communication LTV Channel Model

A complex baseband received signal, $r(t)$, through a wireless mobile communication channel can be modeled[7] as follows [9]:

$$\begin{aligned} r(t) &= \int h(t,\tau)s(t-\tau)\,d\tau + \varepsilon(t) \\ &= \int\int \mathcal{U}(\nu,\tau)s(t-\tau)\,e^{j2\pi\nu t}\,d\tau\,d\nu + \varepsilon(t) \\ &= x(t) + \varepsilon(t) \end{aligned} \tag{25.26}$$

where $h(t,\tau)$ is the channel impulse response representing the LTV behavior; $s(t)$ is the complex baseband transmitted signal; $\varepsilon(t)$ is the additive white Gaussian noise with zero mean and variance σ_ε^2; τ and ν denote the delay and Doppler-shift variables, respectively; and $\mathcal{U}(\nu,\tau)$, the Fourier transform of $h(t,\tau)$ from t to ν, is called the delay-Doppler spread function of the LTV channel. By applying the Fourier transform among the variables t, f, τ, and ν, we can define several system functions [9, 12], with their relationships shown in Figure 25.8, which resembles the dual relationships of time–frequency representations in TFSP, as illustrated by Figure 25.3.

As previously mentioned, the delay–Doppler spread function is often modeled as a wide-sense stationary Gaussian process with uncorrelated scattering [9] whose second-order statistics can be represented by

$$E\{\mathcal{U}(\nu',\tau')\cdot\mathcal{U}^*(\nu,\tau)\} = P_{\mathcal{U}}(\nu,\tau)\cdot\delta(\nu'-\nu)\delta(\tau'-\tau) \tag{25.27}$$

where $P_{\mathcal{U}}(\nu,\tau)$ is the *scattering function* (SF) of the channel. It follows that the WSSUS channel may be represented as a collection of nonscintillating uncorrelated scatterers that cause both multipath delays and Doppler shifts.

[7] In practice, the double integral is bounded by the ranges of multipath delays and Doppler shifts; however, without loss of generality, we use the full range $(-\infty,\infty)$ and drop them for short notation.

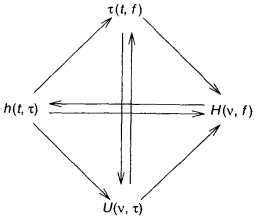

FIGURE 25.8 Relationship among Bello [9] system functions. $\mathcal{T}(t,f)$ and $\mathcal{H}(\nu,f)$ are the time-varying transfer function and output Doppler spread function, respectively.

Restrictions of practical channels on, for instance, time duration, bandwidth, fading rate, delay spread, and Doppler spread, allow a simplified representation of LTV channels in terms of canonical elements. Such channel representations, called *canonical channel* models, can simplify the analysis of the performance of communications systems. A common class of canonical channel representations is the class of sampling models that are applied when a system function vanishes for values of an independent variable (i.e., t, f, τ, or ν) outside some interval or when the input or output time function is time limited or band limited. Various sampling models can be found in [9]. However, we consider here the situation wherein the input signal $s(t)$ is band limited in $[f_o - B_o/2,\ f_o + B_o/2]$ and the output signal $x(t)$ (noise-free) is time limited in $[t_o - T_o/2, t_o + T_o/2]$.

Applying the sampling theorem on both t and f according to the above time and frequency constraints, the received signal may be expressed as [9]

$$x(t) = \sum_m\sum_n \mathcal{U}_{mn}\, s\left(t - \frac{m}{B_o}\right) e^{j2\pi(n/T_o)(t-m/B_o)} \tag{25.28}$$

where

$$\mathcal{U}_{mn} = \frac{1}{T_o B_o}\tilde{\mathcal{U}}\left(\frac{m}{B_o}, \frac{n}{T_o}\right) \tag{25.29}$$

with $\tilde{\mathcal{U}}(\nu,\tau)$ being some smoothed version[8] of $\mathcal{U}(\nu,\tau)$.

When the channel is random, the coefficients $\mathcal{U}_{mn}$ become random variables. Under the WSSUS assumption, the correlation of $\mathcal{U}_{mn}$ can be expressed in terms of the SF, $P_{\mathcal{U}}(\nu,\tau)$. Additionally, if the SF varies very little for changes in τ of the order $1/B_o$ or ν of the order $1/T_o$, this correlation is approximated as

$$E\{\mathcal{U}_{mn}\mathcal{U}_{rs}^*\} = \begin{cases} \frac{1}{T_o B_o} P_{\mathcal{U}}\left(\frac{m}{B_o}, \frac{n}{T_o}\right) & \text{for } m = r,\ n = s \\ 0 & \text{otherwise} \end{cases} \tag{25.30}$$

which means that the delay–Doppler coefficients $\mathcal{U}_{mn}$ are uncorrelated at different values of multipath delays and Doppler shifts. In practice, the multipath-delay τ vanishes outside $[0, T_m]$ and Doppler shift

[8] The expression of $\tilde{\mathcal{U}}(\nu,\tau)$ is given by

$$\tilde{\mathcal{U}}(\nu,\tau) = \int\int e^{j2\pi f_0(\tau-\eta)} e^{-j2\pi t_o(\nu-\mu)}\,\mathrm{sinc}[B_o(\tau-\eta)]\,\mathrm{sinc}[T_o(\nu-\mu)]\,\mathcal{U}(\mu,\eta)\,d\mu\,d\eta$$

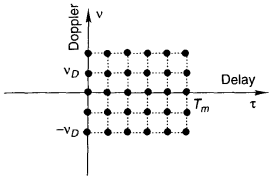

FIGURE 25.9 Second-order statistics of frequency-selective fast fading channel with WSSUS assumption. (T_m and ν_D are the maximum multipath delay and Doppler shift for a particular mobile environment.)

vanishes outside $[-\nu_D, \nu_D]$, where T_m and ν_D are the maximum multipath delay and maximum Doppler shift, respectively. Consequently, the statistics of the WSSUS channel through the above correlation may be sketched on the delay–Doppler plane as shown in Figure 25.9 [26].

We will shortly see how this canonical model can be used to approach the problem of channel estimation. Other issues relating to this model are not reviewed in this chapter but may be of interest, such as multiuser detection in [26] and blind multiuser equalization in [27].

25.3.1.2 Estimation of LTV channels

We review here the problem of pilot-based coherent estimation of LTV channels for CDMA systems using the minimum mean square error (MMSE) approach, which is based on the use of a canonical LTV channel [29]. It is known that RAKE receivers are commonly used for channel equalization as well as signal detection in frequency-selective fading environments such as in CDMA systems. However, in TF-selective fading scenarios, the performance of RAKE receivers is degraded. An extension of the canonical channel model given in Equation 25.28 was proposed in [28] to overcome this problem.

Consider a TF-selective fading environment for which T_m and ν_D denote the maximum multipath delay and Doppler shift, respectively. The transmitted signal $s(t)$ in a DS-CDMA scheme has the duration T and bandwidth B ($B = 1/T_c$, where T_c is the chip duration). The complex baseband signal admits the following canonical representation in terms of fixed multipath delays and Doppler shifts [29]:

$$r(t) \approx \sum_{n=0}^{N} \sum_{k=-K}^{K} \mathcal{U}_{kn}\, \xi_{kn}(t) + \varepsilon(t), \quad 0 < t \le T \tag{25.31}$$

where $N = \lceil T_m B \rceil$ and $K = \lceil T\nu_D \rceil$ denote the numbers of resolvable multipath-delay and Doppler-shift components, respectively, and

$$\xi_{kn}(t) = s(t - n/B) \exp\{j2\pi(k/T)t\}$$

It is seen in Equation 25.31 that $x(t)$ is a linear combination of the set of quasi-orthogonal basis functions[9] $\{\xi_{kn}(t)\}$. In other words, thanks to the canonical representation, the TF-selective fading channel has been decomposed into a bank of $(N + 1)(2K + 1)$ TF-non-selective (flat) fading subchannels. A common approach, then, to the problem of channel estimation is to use matched filtering at the outputs of these subchannels.

Given a frame of $(2I + 1)$ pilot symbols, it is required that we estimate the set of channel coefficients $\{\mathcal{U}_{kn}\}$ at the symbol centered in the considered frame (i.e., at symbol 0). The received signal for the entire

[9]The spreading function $s(t)$ is usually designed so that its nonzero lag correlation coefficients are close to zero.

frame becomes

$$r(t) \approx \sum_{i=-I}^{I} \sum_{n=0}^{N} \sum_{k=-K}^{K} \mathcal{U}_{kn}(i)\, \xi_{kn}(t - iT) + \varepsilon(t) \tag{25.32}$$

The matched-filtered outputs for the entire frame, i.e., $\mathbf{z} = [\mathbf{z}^T(-I), \ldots, \mathbf{z}^T(I)]^T$ with output for each symbol $\mathbf{z}(i) = \langle r(t), \xi(t - iT)\rangle \triangleq \int_{-\infty}^{+\infty} r(t)\xi^*(t - iT)\, dt$, can be expressed as

$$\mathbf{z} = \mathbf{Q}\mathbf{u} + \varepsilon$$

where the channel coefficient vector $\mathbf{u} = [\mathbf{u}(-I)^T \cdots \mathbf{u}(0)^T \cdots \mathbf{u}(I)^T]^T$ with $\mathbf{u}(i) = [\mathcal{U}_{1,1}(i), \ldots, \mathcal{U}_{(2K+1),(N+1)}(i)]^T$; the correlation matrix $\mathbf{Q} = \text{diag}\,(\mathbf{P}, \ldots, \mathbf{P})$ with $\mathbf{P} = \int \xi^*(t - iT)\xi^T(t - iT)\, dt = \int_0^T \xi^*(t)\xi^T(t)\, dt$; $\xi(t)$ being the temporal waveform vector: $\xi(t) = [\xi_{1,1}(t), \ldots, \xi_{(2K+1),(N+1)}(t)]^T$; and the colored Gaussian noise vector $\varepsilon = [\varepsilon(-I)^T \cdots \varepsilon(I)^T]^T$ with each colored Gaussian noise vector $\varepsilon(i) = \langle \varepsilon(t), \xi(t - iT)\rangle$ having the covariance matrix $\mathcal{N}_0\mathbf{P}$.

As mentioned earlier, we need to estimate $\mathbf{u}(0)$. The linear MMSE estimation problem is formulated as

$$\mathbf{L}_{opt} = \underset{\mathbf{L}}{\text{argmin}}\ E\{\|\mathbf{u}(0) - \mathbf{L}^H\mathbf{z}\|^2\} \tag{25.33}$$

The solution of the minimization problem in Equation 25.33 is the Wiener filter given by

$$\mathbf{L}_{opt} = (\mathbf{Q}E\{\mathbf{u}\mathbf{u}^H\} + \mathcal{N}_0\mathbf{I})^{-1}\{\mathbf{u}\mathbf{u}^H(0)\} \tag{25.34}$$

The MMSE channel estimate $\hat{\mathbf{u}}(0) = \mathbf{L}_{opt}^H\mathbf{z}$ is then used for symbol detection using RAKE (or maximum ratio combiner) receiver. For the binary phase shift keying (BPSK) signaling scheme and under the assumption of negligible ISI, the estimated symbols are given by

$$\hat{b}(i) = \text{sign}(\text{real}(\hat{\mathbf{u}}(i)^H\mathbf{z}(i)))$$

More analysis on the estimation performance and practical implementation of the MMSE channel estimate in Equation 25.34 under the assumption of uncorrelated $\mathcal{U}_{kn}$ components in a particular symbol of interest[10] or the assumption of quasi-orthogonality of the basis functions $\{\xi_{kn}(t)\}$ can be found in [29, 30].

25.3.1.3 Estimation of Scattering Function

In certain wireless communications systems, e.g., radar or acoustic communications systems, one is interested in estimating the scattering function that reveals the TF-selective behavior of the fading channel under the WSSUS assumption [31–38]. In the problem of SF estimation, a common approach is to use the input–output relationship, described through the general TFDs [39] as

$$E\{\rho_x(t, f)\} = \rho_s(t, f) \underset{t\ f}{**} P_{\mathcal{U}}(t, f) \tag{25.35}$$

where $\rho_s(t, f)$ is a TFD of the input $s(t)$ and $E\{\rho_x(t, f)\}$ is the expected value of a TFD of the output $x(t)$. In the AF domain, the previous relation becomes

$$E\{\mathcal{A}_x(\nu, \tau)\} = \mathcal{A}_s(\nu, \tau) \cdot R_{\mathbf{T}}(\nu, \tau) \tag{25.36}$$

where $R_{\mathbf{T}}(\nu, \tau)$ is the double Fourier transform of the channel SF $P_{\mathcal{U}}(t, f)$. Since the general AF (GAF), $\mathcal{A}_s(\nu, \tau)$, or general TFD, $\rho_s(t, f)$, includes the expression of the kernel, $g(\nu, \tau)$ (see Figure 25.3), and

[10]Note that the channel coefficients $\mathcal{U}_{kn}$ may be correlated in time across the symbols.

this kernel can be made arbitrary, two general classes of SF estimators were then proposed based on *deconvolution* and *direct implementation*, respectively.

The class of deconvolution estimators is defined based on the division of Equation 25.36 by the GAF of the input signal

$$\hat{P}_{\mathcal{U}}(t,f) \triangleq \mathcal{F}^{-1}_{\nu\to f}\{\mathcal{F}_{\tau\to f}\{\mathcal{A}_x(\nu,\tau)\}/\mathcal{A}_s(\nu,\tau)\} \tag{25.37}$$

Similar to the approach in [35], a zero-division problem in Equation 25.37 is encountered. A classical solution is to threshold the symmetric AF $A_s(\nu,\tau)$ at the points equal to zero (see [35] for more details).

On the other hand, one can choose the kernel $g(\nu,\tau)$ so that the TFD $\rho_s(t,f)$ in Equation 25.35 is impulse-like; the left-hand side of Equation 25.35, then approximates to $P_{\mathcal{U}}(t,f)$. Thus, the other class of SF estimators, namely, direct implementation, can be defined as

$$\hat{P}_{\mathcal{U}}(t,f) \triangleq E\{\rho_x(t,f)\} \tag{25.38}$$

We must note here that an impulse representation in the time–frequency plane does not exist due to the constraint of minimum time–frequency bandwidth according to Heisenberg's uncertainty principle. Therefore, we opt to choose an approximation in the sense of good localization in the time–frequency plane. For example, the TFD kernel may be approximated by the Hermite functions [40], which are defined as

$$g_n(x) = (-1)^n e^{x^2/2}\frac{d^n}{dx^n}e^{-x^2/2} \tag{25.39}$$

25.3.2 Interference Mitigation

25.3.2.1 TV-NBI Suppression in DS-CDMA

Spread-spectrum communication, based on which DS-CDMA is implemented, is known to have the capability of suppressing NBI. However, this NBI suppression becomes ineffective when the interfering signal is too powerful. In some of these cases, the interference immunity can be improved significantly by using signal processing techniques that complement the spread-spectrum modulation [16]. These active suppression techniques not only improve error rate performance, but also lead to an increase in capacity of CDMA cellular systems [41]. There have been several models proposed for narrowband interferers existing in communication channels, such as a deterministic sinusoidal signal [16], an autoregressive-modeled signal [42, 43], and a narrowband digital communications signal [44, 45]. A tremendous amount of research on NBI suppression can be seen in [16, 43, 44, 46–52]. None of these methods, however, is capable of suppressing NBI with time-varying spectral characteristics such as a linear FM signal (chirp signal).

To suppress this type of time-varying NBI (TV-NBI), the IF of the TV-NBI is first estimated using some TFDs; then a time-varying zero filter is used to suppress the interference. The effectiveness of TFDs in providing accurate estimates of the IF has extensively been shown in the literature [2, 4, 53, 54]. Using this approach, the problem of TV-NBI suppression has been carried out in [55–59].

Consider the transmission of a spread-spectrum signal $s(t)$ through an AWGN channel characterized by zero-mean Gaussian random process $\epsilon(t)$ and being interfered with by K different linear FM interferences $\zeta_k(t)$. The received signal model may be expressed in the form

$$r(t) = s(t) + \sum_{k=1}^{K}\zeta_k(t) + \epsilon(t) \tag{25.40}$$

Each interference signal belongs to the class of linear FM signals, with power P_{ζ_k}, that can be expressed as

$$\zeta_k(t) = \sqrt{P_{\zeta_k}}\,e^{j\phi(t,\boldsymbol{\theta}_k)} = \sqrt{P_{\zeta_k}}\,e^{j(2\pi f_k t+\pi g_k t^2)}$$

where $\boldsymbol{\theta}_k = (f_k, g_k)$. The IF of each monocomponent linear FM signal is defined as

$$f_i(t,\boldsymbol{\theta}_k) \triangleq \frac{1}{2\pi}\frac{d\phi(t,\boldsymbol{\theta}_k)}{dt} = f_k + g_k t \tag{25.41}$$

For monocomponent TV-NBI, i.e., $K = 1$, the Born–Jordan distribution and the cone-shape ZAM distribution were used to estimate the IF in [55], and the spectrogram was used in [60, 61]. A problem related to this method is that if the signal-to-interference ratio is high, the estimation of the interference parameters might fail, and the suppression filter could track the useful signal, instead of the interference.

This problem can be improved by using the Wigner–Hough transform [57], defined as [62]

$$WH_r(\boldsymbol{\theta}_k) \triangleq \int_{-\infty}^{\infty} W_r(t, f_i(t;\boldsymbol{\theta}_k))\,dt \tag{25.42}$$

where $W_r(t,f)$ denotes the WVD of $r(t)$ and $f_i(t;\boldsymbol{\theta}_k)$ are the individual IFs of the interferences as given in Equation 25.41. This method also has the ability to deal with multicomponent TV-NBI. The integration in Equation 25.42 over all possible lines of the WVD, which is obtainable by applying a Hough transform, or equivalently, a Radon transform of the WVD, gives rise to peaks in the final parameter space; each peak corresponds to one linear FM signal, whose modulation parameters, (f_k, g_k), are the coordinates of the peaks.

We know that the WVD is optimal in representing monocomponent linear FM signals. The estimation of the IF using the peak of the XWVD achieves the best performance [63]. This technique, therefore, can be effectively used to estimate monocomponent linear FM TV-NBI. For multicomponent TV-NBI, the WVD is not optimal anymore. An alternative solution in this case is to use the BD, in Equation 25.23, since it outperforms some other reduced interference distributions when comparing the capacity of reducing the cross-terms [18].

25.3.2.2 Signal Modulation Design for ISI Mitigation

Apart from the DS-CDMA system mentioned previously, many other CDMA system concepts have been proposed, among which MC-CDMA is a promising system compared to DS-CDMA [15, 64]. MC transmission is a method to design a bandwidth-efficient communication system in the presence of channel distortion (ISI, especially for high-data-rate communications) by dividing the available channel bandwidth into a number of subchannels such that each channel is nearly ideal. The idea of using MC transmission comes from the advantage of this system in overcoming the effect of signal fading on time-varying channels [13]. The typical MC transmission system is the orthogonal frequency division multiplexing (OFDM) system. The combination of OFDM and CDMA allows for optimal detection performance, use of the available spectrum in an efficient way, retention of many advantages of a CDMA system, and exploitation of frequency diversity [65–68].

In MC transmission, the modulation scheme is done based on a set of basis functions (one is a time–frequency-shifted version of another) constructed by Gaussian pulse [69] or Nyquist pulse [70]. These pulses are required to have two important characteristics: (1) orthogonality to avoid ISI and interchannel interference (ICI), and (2) good localization to avoid symbol energy smearing out over the channel and perturbing neighboring symbols. For wireless mobile communication channels with TF-dispersive characteristics, the above two conditions become critical since the localization of the pulses is dispersed. There is a need to design better localized basis functions under such TF-dispersive conditions of the wireless mobile channels, in other words, to design a new set of basis functions so that the effects of ISI and ICI are minimized. The design of different pulses can be carried out using TF analysis in the ambiguity domain, where Hermite pulses have been proved to have better TF localization than Gaussian or Nyquist under TF-dispersive channels [40].

Consider an MC modulation scheme used in such a TF-dispersive mobile channel. Let I be the number of channels in the scheme in which $f_{c_i} = i\Delta f_c$ $(i = 0, \ldots, I-1)$ is the set of carrier frequencies and Δf_c is the spacing between adjacent carriers (usually $\Delta f_c \le W$, where W is the bandwidth of the signal).

The transmitted signal is given by

$$x(t) = \sum_{i=0}^{I-1} \sum_{n=-\infty}^{\infty} c_{n,i}\, \xi_{n,i}(t) \tag{25.43}$$

where $c_{n,i}$ are the information-bearing symbols and $\xi_{n,i}$ are the basis functions, defined as

$$\xi_{n,i}(t) = \lambda(t - nT)\, e^{j2\pi f_i t} \tag{25.44}$$

The envelope function $\lambda(t)$ is called an elementary pulse (T being the symbol duration). Demodulation is performed by a projection of the received signal on the complex conjugates of the basis functions

$$r_{p,q} = \int r(t)\, \xi^*_{p,q}(t)\, dt \tag{25.45}$$

The orthogonality condition requires

$$\int \xi_{n,i}(t)\, \xi^*_{p,q}(t)\, dt = \int \lambda(t)\lambda^*(t + (n-p)T)\, e^{-j2\pi(i-q)\Delta f_i t}\, dt =$$

$$= \delta_{n,p}\delta_{i,q} = \begin{cases} 1 & n = p \text{ and } i = q \\ 0 & \text{otherwise} \end{cases} \tag{25.46}$$

By noting that the integral in Equation 25.46 can be considered a sampling of the AF, $\mathcal{A}_\lambda(\nu, \tau)$ (a shifted version of the symmetrical AF defined in Equation 25.17 of the envelope function $\lambda(t)$), Equation 25.46 can be expressed as

$$\int \xi_{n,i}(t)\, \xi^*_{p,q}(t)\, dt = \mathcal{A}_\lambda((i-q)\Delta f_c, (n-p)T)$$

The second required condition is good localization in the sense of a minimum energy spread in order to avoid the symbol energy smearing out over the dispersive channel and perturbing neighboring symbols. If ΔT and ΔW represent the time dispersion and frequency dispersion,[11] respectively, the following conditions need to be verified so the channel can be considered as frequency-non-selective and slow fading for each carrier:

$$\nu_D \ll \Delta f_c \qquad \Delta W \ll B_{coh}$$
$$T_m \ll T \qquad \Delta T \ll T_{coh}$$

where $B_{coh} \approx 1/T_m$ and $T_{coh} \approx 1/\nu_D$ are the coherence bandwidth and coherence time, respectively.

Several drawbacks of the Nyquist or Gaussian pulse, being the elementary pulse due to the lack of orthogonality and localization in TF-dispersive channels, lead to the design of a new pulse [40] based on the Hermite function given by (Equation 25.39).

Orthogonality is optimized by evaluating the AF of $\lambda(t)$, where $\lambda(t)$ is a linear combination of $D_{4n}(t) = f_{4n}(\sqrt{2\pi}t)$, as given by

$$\lambda(t) = \sum_{k=0}^{N_F-1} F_{4k} D_{4k}(t)$$

where N_F is the number of coefficients F_{4k} that can be found when imposing the condition for orthogonality.

[11] ΔT and ΔW are defined as $(\Delta T)^2 = \int t^2 |\lambda(t)|^2\, dt$ and $(\Delta W)^2 = \int f^2 |\Lambda(f)|^2\, df$ ($\Lambda(f)$ being the FT of $\lambda(t)$).

Performance evaluation shows that the Hermite pulse is better than the Nyquist pulse with cosine roll-off for a channel with characteristics of $T_m \leq 0.01$ and $\nu_D \leq 0.01$. The Hermite pulse loses its advantages at around $\nu_D = 0.1$. However, better performance of the Hermite pulse in the presence of time dispersion is encouraging for its application in multiuser multicarrier systems where different users are transmitting on neighboring carriers.

25.3.2.3 Multiple-Access Interference in MC-CDMA

Also based on the use of the ambiguity domain, a design of new signature waveforms for the MC-CDMA system was proposed in [71]. In MC-CDMA, the signature waveforms are normally designed in the frequency domain, whereas in DS-CDMA, they are designed in the time domain. There exist two major problems for multiuser access in an MC system: (1) the high effort in signal processing due to the need of a complex-valued RAKE or multiuser detector [73], and (2) the design of optimized code sets with reduced dynamic range and proper autocorrelation and cross-correlation properties. A possibility to the orthogonalized codes by shifting the signal in frequency has been shown in [72]. Consequently, a K-users-1-code MC-CDMA system was proposed in [71]. To each user, the same code is assigned with different frequency shifts.

More precisely, consider a multicarrier spread-spectrum signal defined as

$$s(t) = b(t) \cdot \sum_{q=0}^{Q-1} c(q)\, e^{j2\pi q t/T} = b(t) \cdot c_0(t)$$

where $b(t)$ is the data signal, $c(q)$ are the complex code coefficients in the frequency domain, and Q is the spreading factor. The transmitted signal of the kth user is shifted from that of the first user as

$$s_k(t) = b_k(t) \cdot \sum_{q=0}^{Q-1} c(q)\, e^{j2\pi(q+k)t/T} = b_k(t) \cdot c_0(t) e^{j2\pi kt/T} = b_k(t) \cdot c_k(t)$$

Due to the multipath fading, the received signal for the up-link of K users is given by

$$r(t) = \sum_{k=0}^{K-1} \sum_{p=0}^{P-1} \alpha_{k,p}(t)\, b_k(t - \tau_{k,p})\, c_k(t - \tau_{k,p})\, e^{j2\pi \nu_k t/T} + \epsilon(t)$$

where P is the number of propagation paths (assuming the same for all users) and $\alpha_{k,p}(t)$, $\tau_{k,p}$, and ν_k are the attenuation, multipath delay, and Doppler shift of the kth user's signal, respectively.

Using a time domain RAKE receiver with ideal path synchronization, we get as an expression for the detected symbol $\hat{b}_{k,p}$ of user k in path p

$$\hat{b}_{k,p} = \frac{1}{T} \int_0^T r(t) c^*_k(t - \tau_{k,p})\, dt$$

The detection problem can be simplified to analyzing the correlation functions $\mathcal{A}_{k_1,k_2}(\nu, \tau)$, which depend on the data signal $b(t)$ and the code $c(t)$. The whole interference could be evaluated by summing these terms, $\mathcal{A}_{k_1,k_2}(\nu, \tau)$, for all users and all paths with the correct path weight. Without loss of generality, choosing $k_1 = 1$ and $k_2 = k$, we have

$$\mathcal{A}_{1,k}(\nu_k, \tau_k) = \frac{1}{T} \int_0^T s_k(t) s^*_1(t - \tau_k)\, e^{j2\pi \nu_k t/T}\, dt \tag{25.47}$$

which is a representation of the signal in the ambiguity domain. By not considering the influence of the

data signal, Equation 25.47 becomes

$$\mathcal{A}_{0,k}(\nu_k,\tau_k)=\sum_{n_1=0}^{Q-1}\sum_{n_2=0}^{Q-1}c(n_1)c^*(n_2)\,e^{j2\pi[n_2(\tau_k/T-1)+n_1+k+\nu_k]}\times \mathrm{sinc}[\pi(n_1-n_2+k+\nu_k)]$$

In the ambiguity domain, the values outside $\mathcal{A}_{1,k}(0,0)$ could be considered interference values of a user with delay $\tau=\tau_k$ and frequency shift $\nu=(k+\nu_k)/T$ to user 1. In other words, we have imperfect time and frequency synchronization.

Assuming that the delay τ and frequency deviation ν are uniformly distributed over $(0,T)$ and $(-\nu_k,\nu_k)$, respectively, the mean interference value is given by

$$\langle|\mathcal{A}_{1,k}(\tau_k,\nu_k)|^2\rangle=\frac{1}{2\nu_k}\int_0^T\int_{(k-\nu_k)/T}^{(k+\nu_k)/T}|\mathcal{A}(\nu,\tau)+\mathcal{A}^*(\nu,\tau-T)|^2\,d\tau d\nu \tag{25.48}$$

Numerical evaluation shows that codes with more concentrated interference power have a better mean interference and a better performance in the whole system.

In the above section, TFSP has been considered for one-dimensional signals. In the next section, TFDs are applied to multidimensional signals provided by multiantennae in order to solve relevant problems that arise in wireless communications.

25.4 Time–Frequency Array Signal Processing

Conventional array signal processing algorithms assume stationary signals and mainly employ the covariance matrix of the data array. When the frequency content of the measured signals is time varying (i.e., nonstationary signals), this class of approaches can still be applied. However, the achievable performances in this case are reduced with respect to those that would be achieved in a stationary environment. In the last decades, the stationarity hypothesis was motivated by the crucial need in practice of estimating sample statistics by resorting to temporal averaging under the additional assumption of ergodic signals. Instead of considering the nonstationarity as a shortcoming and trying to design algorithms robust with respect to nonstationarity, it would be better to take advantage of the nonstationarity by considering it as a source of information. The latter can then be exploited in the design of efficient algorithms in such nonstationary environments.

The question now is, How can we exploit the nonstationarity in array processing? This can be done by resorting to the spatial time–frequency distributions (STFDs), which are a generalization of the TFDs to a vector of multisensor signals (see Figure 25.10). Under a linear model, the STFDs and the commonly known covariance matrix exhibit the same eigenstructure. In wireless communications involving multiantennae, the aforementioned structure is often exploited to estimate some signal parameters through subspace-based techniques.

Algorithms based on STFDs properly use the time–frequency information to significantly improve performance. This improvement comes essentially from the fact that the effects of spreading the noise power while localizing the source energy in the time–frequency domain increase the signal-to-noise ratio (SNR).

STFD-based algorithms exploit the time–frequency representation of the signals together with the spatial diversity provided by the multiantennae.

The concept of the STFD was introduced for the first time in 1996 [75]. It was used successfully in solving the problem of the blind separation of nonstationary signals [75–78]. This concept was then applied to solve the problem of direction-of-arrival (DOA) estimation [79]. Since then, several works were conducted in this area using the new concept of STFD [80–89].

The following notations are used throughout the rest of this chapter. For a given matrix $\mathbf{A}$, the symbols $\mathbf{A}^T$, $\mathbf{A}^*$, $\mathbf{A}^H$, $\mathbf{A}^\#$, trace($\mathbf{A}$), and norm($\mathbf{A}$) respectively denote the transpose, conjugate, conjugate transpose, Moore–Penrose pseudoinverse, trace, and (Euclidean) norm of $\mathbf{A}$.

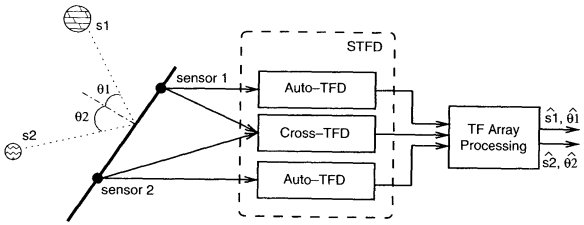

FIGURE 25.10 Time–frequency array signal processing.

25.4.1 The Spatial Time–Frequency Distributions

Given an analytic vector signal $\mathbf{z}(t)$, the spatial instantaneous autocorrelation function is defined as

$$\mathbf{K}_{\mathbf{zz}}(t,\tau)=\mathbf{z}\left(t+\frac{\tau}{2}\right)\mathbf{z}^H\left(t-\frac{\tau}{2}\right) \tag{25.49}$$

Define also the smoothed spatial instantaneous autocorrelation function as

$$\mathbf{S}_{\mathbf{zz}}(t,\tau)=G(t,\tau)\underset{t}{*}\mathbf{K}_{\mathbf{zz}}(t,\tau) \tag{25.50}$$

where $G(t,\tau)$ is some time-lag kernel. The time convolution operator $\underset{t}{*}$ is applied to each entry of the matrix $\mathbf{K}_{\mathbf{zz}}(t,\tau)$. The class of quadratic STFDs then defined as

$$\mathbf{D}_{\mathbf{zz}}(t,f)=\mathcal{F}_{\tau\to f}\{\mathbf{S}_{\mathbf{zz}}(t,\tau)\} \tag{25.51}$$

where the Fourier transform $\mathcal{F}$ is applied to each entry of the matrix $\mathbf{S}_{\mathbf{zz}}(t,\tau)$.

The discrete-time definition equivalent to Equations 25.50 and 25.51 leads to the simple implementation of STFD and is expressed as

$$\mathbf{D}_{\mathbf{zz}}(n,k)=\mathcal{DF}_{m\to k}\{G(n,m)\underset{n}{\star}\mathbf{K}_{\mathbf{zz}}(n,m)\} \tag{25.52}$$

which can also be expressed as

$$\mathbf{D}_{\mathbf{zz}}(n,k)=\sum_{m=-M}^{M}\sum_{p=-M}^{M}G(p-n,m)\mathbf{z}(p+m)\mathbf{z}^H(p-m)e^{-j4\pi\frac{mk}{N}} \tag{25.53}$$

where the discrete Fourier transform $\mathcal{DF}$ and the discrete-time convolution operator $\underset{n}{\star}$ are applied to each entry of the matrix $G(n,m)\underset{n}{\star}\mathbf{K}_{\mathbf{zz}}(n,m)$ and matrix $\mathbf{K}_{\mathbf{zz}}(n,m)$, respectively.

Note that the STFD of a vector signal is a matrix whose diagonal entries are the classical auto-TFDs of the vector components, and the off-diagonal entries are the cross-TFDs.

A more general definition of the STFD can be given as

$$\mathbf{D}_{\mathbf{zz}}(n,k)=\sum_{m=-M}^{M}\sum_{p=-M}^{M}\mathbf{G}(p-n,m)\odot(\mathbf{z}(p+m)\mathbf{z}^H(p-m)e^{-j4\pi\frac{mk}{N}}) \tag{25.54}$$

where $\odot$ designates the Hadamard product and $[\mathbf{G}(n,m)]_{ij}=G_{ij}(n,m)$ is the time-lag kernel associated with the pair of sensor signals $z_i(n)$ and $z_j(n)$ (kernels G_{ij} might be chosen according to the nature of considered signals $z_i(n)$ and $z_j(n)$ if such *a priori* information is available).

25.4.1.1 Structure under linear model

Consider the following linear model of the vector signal $\mathbf{z}(n)$:

$$\mathbf{z}(n) = \mathbf{A}\mathbf{s}(n) \tag{25.55}$$

where $\mathbf{A}$ is a $K \times L$ matrix ($K \geq L$) and $\mathbf{s}(n)$ is a $L \times 1$ vector, which is referred to as the source signal vector.

Under this linear model the STFDs take the following structure:

$$\mathbf{D}_{zz}(n,k) = \mathbf{A}\mathbf{D}_{ss}(n,k)\mathbf{A}^H \tag{25.56}$$

where $\mathbf{D}_{ss}(n,k)$ is the source STFD of vector $\mathbf{s}(n)$ whose entries are the auto- and cross-TFDs of the source signals.

The auto-STFD denoted by $\mathbf{D}^a_{zz}(n,k)$ is the STFD, $\mathbf{D}_{zz}(n,k)$, evaluated at autoterm points only. Correspondingly, the cross STFD $\mathbf{D}^c_{zz}(n,k)$ is the STFD, $\mathbf{D}_{zz}(n,k)$, evaluated at cross-term points.

Note that the diagonal (off-diagonal) elements of $\mathbf{D}_{ss}(n,k)$ are autoterms (cross-terms). Thus, the auto- (cross-) STFD $\mathbf{D}^a_{ss}(n,k)$ ($\mathbf{D}^c_{ss}(n,k)$) is diagonal (off-diagonal[12]) for each time–frequency point that corresponds to a source autoterm (cross-term), provided the window effect is neglected.

25.4.1.2 Structure under Unitary Model

Denote by $\mathbf{W}$ a $L \times K$ whitening matrix such that

$$(\mathbf{WA})(\mathbf{WA})^H = \mathbf{U}\mathbf{U}^H = \mathbf{I} \tag{25.57}$$

Pre- and postmultiplying the STFD $\mathbf{D}_{zz}(n,k)$ by $\mathbf{W}$ leads to the whitened STFD, defined as

$$\underline{\mathbf{D}}_{zz}(n,k) = \mathbf{W}\mathbf{D}_{zz}(n,k)\mathbf{W}^H = \mathbf{U}\mathbf{D}_{ss}(n,k)\mathbf{U}^H \tag{25.58}$$

where the second equality stems from the definition of $\mathbf{W}$ and Equation 25.56. This above whitening leads to a linear model with a unitary mixing matrix.

Note that the whitening matrix can be computed in different ways. It can be obtained, for example, as an inverse square root of the observation covariance matrix [78] or computed from the STFD matrices as shown in [90].

At autoterm points, the whitened auto-STFD has the following structure:

$$\underline{\mathbf{D}}_{zz}(n,k) = \mathbf{U}\mathbf{D}^a_{ss}(n,k)\mathbf{U}^H \tag{25.59}$$

where $\mathbf{D}^a_{ss}(n,k)$ is diagonal. However, at cross-term points, the whitened cross STFD exhibits the following structure:

$$\underline{\mathbf{D}}_{zz}(n,k) = \mathbf{U}\mathbf{D}^c_{ss}(n,k)\mathbf{U}^H \tag{25.60}$$

where $\mathbf{D}^c_{ss}(n,k)$ is off-diagonal.

The above-defined STFDs permit the application of subspace techniques to solve a large class of channel estimation and equalization, blind source separation, and high-resolution DOA estimation problems. For the blind source separation problem, the STFDs allow the separation of Gaussian sources with identical spectral shape but with different time–frequency signatures [78]. In the area of DOA finding, the estimation of the signal and noise subspaces from the STFDs highly improves the angular resolution performance.

[12] A matrix is off-diagonal if its diagonal entries are zeros.

25.4.2 STFD Structure in Wireless Communications

In wireless communications, when L user signals arrive at a K-element antenna, the linear data model

$$\mathbf{z}(n) = \mathbf{A}\mathbf{s}(n) + \mathbf{n}(n) \tag{25.61}$$

is commonly assumed, where we recall that $\mathbf{z}(n)$ is the $K \times 1$ data vector received at the antennae and $\mathbf{s}(n)$ is the $L \times 1$ user data vector, the spatial matrix $\mathbf{A} = [\mathbf{a}_1 \cdots \mathbf{a}_n]$ represents the propagation matrix,[13] $\mathbf{a}_i$ is the steering vector corresponding to the ith user, and $\mathbf{n}(n)$ is an additive noise vector whose entries are modeled as stationary, temporally and spatially white, zero-mean random processes, and independent of the user-emitted signals.

Under the above assumptions, the expectation of the TFD matrix between the user signal and the noise vectors vanishes, i.e.,

$$E\{\mathbf{D}_{sn}(n,k)\} = 0 \tag{25.62}$$

and it follows that

$$\bar{\mathbf{D}}_{zz}(n,k) = \mathbf{A}\bar{\mathbf{D}}_{ss}(n,k)\mathbf{A}^H + \sigma^2\mathbf{I} \tag{25.63}$$

with

$$\bar{\mathbf{D}}_{zz}(n,k) = E\{\mathbf{D}_{zz}(n,k)\} \tag{25.64}$$

$$\bar{\mathbf{D}}_{ss}(n,k) = E\{\mathbf{D}_{ss}(n,k)\} \tag{25.65}$$

where σ^2 is the noise power and $\mathbf{I}$ is the identity matrix. Under the same assumptions, the data covariance matrix, which is commonly used in array signal processing, is given by

$$\mathbf{R}_{zz} = \mathbf{A}\mathbf{R}_{ss}\mathbf{A}^H + \sigma^2\mathbf{I} \tag{25.66}$$

where

$$\mathbf{R}_{zz} = E\{\mathbf{z}(n)\mathbf{z}(n)^H\} \tag{25.67}$$

$$\mathbf{R}_{ss} = E\{\mathbf{s}(n)\mathbf{s}(n)^H\} \tag{25.68}$$

From Equations 25.63 and 25.66, it becomes clear that the STFDs and the covariance matrix exhibit the same eigenstructure. This structure is often exploited to estimate some signal parameters through subspace-based techniques.

25.4.3 Advantages of STFDs over Covariance Matrix

The STFDs allow the processing of the received data in both the spatial domain and the two-dimensional time–frequency domain simultaneously. In time–frequency array signal processing, the STFDs are eigendecomposed, instead of the traditional covariance matrix $\mathbf{R}_{zz}$, to separate the signal subspace and noise subspace. Thanks to the availability of time-varying filtering in the time–frequency domain, the STFD-based approaches can handle signals corrupted by interference occupying the same frequency band or the same time slot, but with different time–frequency signatures; thus, signal selectivity is increased with respect to covariance matrix-based methods. In addition, the effect of spreading noise power while localizing the user energy in the time–frequency plane amounts to increased robustness of the STFD-based approaches with respect to noise. In other words, the eigenvectors of the signal subspace obtained from an STFD matrix that is made up of signal autoterms are more robust to noise than those obtained from the

[13] This matrix is also known as the mixing matrix.

covariance matrix. Hence, the performance of the STFD-based approaches can be significantly improved, particularly when the input SNR is low[14] (typically, an SNR of 0 dB or lower). Moreover, in [86] it is proved that the traditional covariance-based subspace methods are low-dimensional cases of the STFD subspace methods.

If one selects the kernel $G(n,m)$ in Equation 25.53 so that the corresponding TFD satisfies the marginal condition

$$\sum_k \bar{D}_{z_i z_j}(n,k) = E\{z_i(n) z_j(n)^*\} \tag{25.69}$$

then

$$\sum_k \bar{\mathbf{D}}_{\mathbf{zz}}(n,k) = E\{\mathbf{z}(n)\mathbf{z}(n)^H\} = \mathbf{R}_{\mathbf{zz}} \tag{25.70}$$

The above equation shows that the projection of the STFD over the time domain is nothing more than the traditional covariance matrix. Hence, the space spanned by $\mathbf{R}_{\mathbf{zz}}$ is the projection of the space spanned by $\bar{\mathbf{D}}_{\mathbf{zz}}(n,k)$ over the space that is orthogonal to the frequency dimension. This means that the space spanned by $\bar{\mathbf{D}}_{\mathbf{zz}}(n,k)$ is the extension of the space spanned by $\mathbf{R}_{\mathbf{zz}}$ toward a higher-dimension space. Therefore, the $\mathbf{R}_{\mathbf{zz}}$-based techniques can be seen as a low-dimension special case of the $\bar{\mathbf{D}}_{\mathbf{zz}}(n,k)$-based ones. This is quite straightforward since the STFD-based methods are multidimensional (spatial–time–frequency) processing methods. Obviously, the details and signatures of the signal will be described more accurately and finely in higher-dimension space. In fact, this is the reason that the STFD-based methods have better performance, such as signal selectivity, interference suppression, and high resolution, over the conventional covariance matrix-based approaches.

25.4.4 Selection of Autoterms and Cross-Terms in the Time–Frequency Domain

STFD-based methods require computation of STFDs at different time–frequency points. At autoterm points, where the diagonal structure of the source STFD is enforced, the data STFDs are either incorporated into a joint diagonalization (JD) technique or eigendecomposed after simple averaging over the source signatures of interest to estimate the mixing, or the array manifold matrix. At cross-term points, where this time the off-diagonal structure of the source STFD is enforced, the data STFDs are incorporated in an off-diagonalization technique to achieve the task of the mixing/propagation matrix identification.

An intuitive procedure to select the autoterms is to consider the time–frequency points corresponding to the maximum energy in the time–frequency plane [75]. The above intuitive procedure has shown some limitations in practical situations. A projection-based selection procedure of cross-terms and autoterms has been proposed in [83]. The latter exploits the off-diagonal structure of the cross-source STFDs and proceeds on whitened data STFDs. More precisely, for a cross-source STFD, we have

$$\text{Trace}(\underline{\mathbf{D}}^c_{\mathbf{zz}}(n,k)) = \text{Trace}(\mathbf{U}\mathbf{D}^c_{\mathbf{ss}}(n,k)\mathbf{U}^H) = \text{Trace}(\mathbf{D}^c_{\mathbf{ss}}(n,k)) \approx 0 \tag{25.71}$$

Based on this observation, the following testing procedure applies:

$$\text{if } \frac{\text{Trace}\{\underline{\hat{\mathbf{D}}}_{\mathbf{zz}}(n,k)\}}{\text{norm}\{\underline{\hat{\mathbf{D}}}_{\mathbf{zz}}(n,k)\}} < \epsilon \rightarrow \text{decide that } (n,k) \text{ is a cross-term point}$$

where the threshold ϵ is a positive scalar (typically $\epsilon = 0.9$). In the underdetermined case (i.e., $K < L$), the matrix $\mathbf{U}$ (see Section 25.4.1.2) is nonsquare (with more columns than rows), and consequently, $\mathbf{U}^H\mathbf{U} \neq \mathbf{I}$

[14] Subspace analysis of the STFDs vs. the covariance matrix is provided in [82].

represents the projection matrix onto the row space of $\mathbf{U}$. Therefore, Equation 25.71 becomes only an approximation. An alternative solution consists of exploiting the existence of only one source at some autoterm points. At such points, each autoterm STFD matrix is of rank one, or at least has one large eigenvalue compared to its other eigenvalues. Therefore, one can use rank selection criteria, such as MDL (minimum description length) or AIC (Akaike information criterion) [91], to select autoterm points as those corresponding to STFD matrices of selected rank equal to one. For simplicity, the following criterion can be used:

$$\text{if } \left| \frac{\lambda_{\max}\{\hat{\mathbf{D}}_{\mathbf{zz}}(n,k)\}}{\text{norm}\{\hat{\mathbf{D}}_{\mathbf{zz}}(n,k)\}} - 1 \right| > \epsilon \rightarrow \text{decide that } (n,k) \text{ is a cross-term point}$$

where ϵ is a small positive scalar (typically, $\epsilon =$ 1E-4) and $\lambda_{\max}\{\hat{\mathbf{D}}_{\mathbf{zz}}(n,k)\}$ represents the largest eigenvalue of $\hat{\mathbf{D}}_{\mathbf{zz}}(n,k)$.

A statistical test to decide whether a time–frequency point is dominated by auto- or cross-terms is proposed in [92]. The latter consider the following test statistic:

$$\frac{\text{Trace}\{\underline{\hat{\mathbf{D}}}_{\mathbf{zz}}(n,k)\}}{\text{norm}\{\underline{\hat{\mathbf{D}}}_{\mathbf{zz}}(n,k)\}} \tag{25.72}$$

To discriminate between noise and either auto- or cross-term, the variance of the test statistic is used. Because only a single value of the test statistic is known at the time–frequency point under test, the variance is estimated using a bootstrap resampling technique [88, 92]. Once the noise regions in the time–frequency domain are identified, a threshold is set to distinguish the autoterms from the cross-terms. In [93], array averaging of the STFDs is used to reduce the cross-terms without smearing the autoterms, allowing the autoterms to be more pronounced and easier to detect in the time–frequency plane.

In [94], it is shown that for real-valued signals, the imaginary parts of the STFDs, when not equal to zero, only correspond to cross-terms whatever the considered point in the time–frequency plane. This result was exploited to derive a criterion for the auto- and cross-term selection. In the case of noisy signals, reference [85] describes a detection criteria of cross- and auto-terms in the time–frequency plane by introducing two thresholds based on the Bayesian and Neyman–Pearson approaches.

The selection of autoterms in the time–frequency domain is still an open problem. And the success of any STFD-based technique depends highly on the performance of the employed autoterm selection procedure.

25.4.5 Time–Frequency Direction-of-Arrival Estimation

In order to obtain the mobile users' spatial information and achieve the space-division multiple access (SDMA), the DOA estimation of far field sources from the multiantenna outputs is one of the important issues in next-generation wireless communications. Thanks to their super resolution and robustness, the subspace-based methods, such as MUSIC [95] and ESPRIT [96], are considered the most popular techniques in traditional array processing. However, all these subspace methods assume the signals impinged on the antennae stationary, while typical signals in wireless communications, such as frequency-hopping signals or frequency-modulated signals, are nonstationary with some *a priori* known information on their time-varying frequency content. In addition, several nonspatial features such as time and frequency signatures of the signals are ignored in conventional methods. These defects may result in unaffordable estimation error.

In most wireless communications systems, the signals are man-made and hence much information contained in these signals is known or can be obtained *a priori*. One can exploit this information not only in the spatial domain but also in the time–frequency domain in order to improve the performance. One of these techniques is the STFD-based DOA estimation method. Recently, several traditional DOA estimation techniques have been extended to nonstationary signals thanks to the use of STFD instead of the covariance matrix. Hence, time–frequency MUSIC (TF-MUSIC) was first introduced in [79]; then time–frequency maximum likelihood (TF-ML), time–frequency signal subspace fitting (TF-SSF), and time–frequency

ESPRIT (TF-ESPRIT) were introduced in [97], [86], and [89], respectively. Below, we describe only TF-MUSIC as an illustrative example on how the STFDs can be exploited for DOA estimation.

25.4.5.1 Data Model

Consider again Equation 25.61, which is often encountered in wireless communications:

$$\mathbf{z}(n) = \mathbf{A}(\theta)\mathbf{s}(n) + \mathbf{n}(n) \tag{25.73}$$

Herein, the propagation matrix $\mathbf{A}(\theta) = [\mathbf{a}(\theta_1), \ldots, \mathbf{a}(\theta_L)]^T$, also known as steering matrix, is parameterized by the parameter vector $\theta = [\theta_1, \ldots, \theta_L]^T$, where $\mathbf{a}(\theta_k)$ and θ_k define the steering vector and the DOA of the kth user, respectively.

Assuming a noise-free environment, the structure of the STFD associated with the above model is given by

$$\mathbf{D}_{zz}(n,k) = \mathbf{A}(\theta)\mathbf{D}_{ss}(n,k)\mathbf{A}(\theta)^H \tag{25.74}$$

25.4.5.2 TF-MUSIC

By performing the singular value decomposition (SVD) of the steering matrix,

$$\mathbf{A}(\theta) = [\mathbf{E}_s \mathbf{E}_n][\mathbf{D} \;\; \mathbf{0}]^T \mathbf{V}^H \tag{25.75}$$

and incorporating the results in Equation 25.74, it is easily shown that

$$\mathbf{D}_{zz}(n,k) = [\mathbf{E}_s \mathbf{E}_n]\mathbf{D}(n,k)[\mathbf{E}_s \mathbf{E}_n]^H \tag{25.76}$$

where $\mathbf{D}(n,k)$ is a block-diagonal matrix given by

$$\mathbf{D}(n,k) = \mathrm{diag}[\mathbf{D}\mathbf{V}^H \mathbf{D}_{ss}(n,k)\mathbf{V}\mathbf{D} \;\; \mathbf{0}] \tag{25.77}$$

Since $\mathbf{E}_s$ and $\mathbf{E}_n$, which span the signal subspace and noise subspace, respectively, are fixed and independent of the time–frequency point (n,k), Equation 25.76 reveals that any matrix $\mathbf{D}_{zz}(n,k)$ is block-diagonalized by the unitary transform $\mathbf{E} = [\mathbf{E}_s \; \mathbf{E}_n]$.

A simple way to estimate $\mathbf{E}_s$ and $\mathbf{E}_n$ is to perform the SVD on a single matrix $\mathbf{D}_{zz}(n,k)$ or an averaged version of $\mathbf{D}_{zz}(n,k)$ over the source signatures of interest. But indeterminacy arises in the case where $\mathbf{D}_{ss}(n,k)$ is singular. To avoid this problem, a joint block diagonalization (JBD) of the combined set of $\{\mathbf{D}_{zz}(n_l,k_l)|l = 1,\ldots,P\}$ can be performed by exploiting the joint structure (Equation 25.76) of the STFDs. This JBD is achieved by the maximization under unitary transform of the following criterion:

$$C(\mathbf{U}) \triangleq \sum_{l=1}^{P}\sum_{i,j=1}^{L} \left|\mathbf{u}_i^H \mathbf{D}_{zz}(n_l,k_l)\mathbf{u}_j\right|^2 \tag{25.78}$$

over the set of unitary matrices $\mathbf{U} = [\mathbf{u}_1,\ldots,\mathbf{u}_K]$. Note that in [98], an efficient algorithm for solving Equation 25.78 exists. Once the signal and noise subspaces are estimated, one can use any subspace-based technique to estimate the DOAs. The MUSIC algorithm [95] is then applied to the noise subspace matrix $\hat{\mathbf{E}}_n$ estimated from Equation 25.78. Hence, the TF-MUSIC algorithm estimates the DOAs by finding the L largest peaks of the localization function

$$f(\theta) = \left|\hat{\mathbf{E}}_n^H \mathbf{a}(\theta)\right|^{-2} \tag{25.79}$$

25.4.6 Time–Frequency Source Separation

Currently, blind source separation is considered one of most promising techniques in wireless communications and more specifically in multiuser detection. The underlying problem consists of recovering the original waveforms of the user-emitted signals without any knowledge on their linear mixture. This mixture can be either instantaneous or convolutive. The problem of blind source separation has two inherent indeterminacies such that source signals can only be identified up to a fixed permutation and some complex factors [99].

So far, the problem of blind source separation has been solved using statistical information available on the source signals. The first solution was based on the cancellation of higher-order moments assuming non-Gaussian and independent and identically distributed (i.i.d.) signals [100]. Other solutions based on minimization of cost functions, such as contrast functions [101] or likelihood function [102], have been proposed. In the case of non-i.i.d. signals and even Gaussian sources, solutions based on second-order statistics were also proposed [99].

When the frequency content of the source signals is time varying, one can exploit the powerful tool of the STFDs to separate and recover the incoming signals. In this context, the underlying problem can be regarded as signal synthesis from the time–frequency plane with the incorporation of the spatial diversity provided by the antennae.

In contrast to conventional blind source separation approaches, the STFD-based signal separation techniques allow separation of Gaussian sources with identical spectral shape provided that the sources have different time–frequency signatures. Below, we describe applications of the STFDs for the separation of both instantaneous and convolutive mixtures.

25.4.6.1 Separation of Instantaneous Mixture

The multiantenna signal $\mathbf{z}(n)$ is assumed to be nonstationary and to obey the linear model in Equation 25.55. The problem under consideration consists of identifying the matrix $\mathbf{A}$ and recovering the source signals $\mathbf{s}(n)$ up to a fixed permutation and some complex factors.

By selecting autoterm points, the whitened auto-STFDs have the structure in Equation 25.59 that we recall herein:

$$\underline{\mathbf{D}}_{zz}(n,k) = \mathbf{U}\mathbf{D}_{ss}^a(n,k)\mathbf{U}^H \tag{25.80}$$

with $\mathbf{D}_{ss}^a(n,k)$ a diagonal matrix. The missing unitary matrix $\mathbf{U}$ is retrieved up to permutation and phase shifts by JD of a combined set $\{\underline{\mathbf{D}}_{zz}(n_a,k_a)|a = 1,\ldots,P\}$ of P auto-STFDs. The incorporation of several autoterm points in the JD reduces the likelihood of having degenerate eigenvalues and increases robustness to a possible additive noise. The above JD is defined as the maximization of the following criterion:

$$C_{JD}(\mathbf{V}) \triangleq \sum_{a=1}^{P}\sum_{i=1}^{L} \left|\mathbf{v}_i^H \underline{\mathbf{D}}_{zz}(n_a,k_a)\mathbf{v}_i\right|^2 \tag{25.81}$$

over the set of unitary matrices $\mathbf{V} = [\mathbf{v}_1,\ldots,\mathbf{v}_L]$.

The selection of cross-term points leads to the whitened cross STFD (Equation 25.60),

$$\underline{\mathbf{D}}_{zz}(n,k) = \mathbf{U}\mathbf{D}_{ss}^c(n,k)\mathbf{U}^H \tag{25.82}$$

with $\mathbf{D}_{ss}^c(n,k)$ an off-diagonal matrix. The unitary matrix $\mathbf{U}$ is found up to permutation and phase shifts by joint off-diagonalization (JOD) of a combined set $\{\underline{\mathbf{D}}_{zz}(n_c,k_c)|c = 1,\ldots,Q\}$ of Q cross-STFDs. This JOD is defined as the maximization of the following criterion:

$$C_{JOD}(\mathbf{V}) \triangleq -\sum_{c=1}^{Q}\sum_{i=1}^{L} \left|\mathbf{v}_i^H \underline{\mathbf{D}}_{zz}(n_c,k_c)\mathbf{v}_i\right|^2 \tag{25.83}$$

over the set of unitary matrices $\mathbf{V} = [\mathbf{v}_1,\ldots,\mathbf{v}_L]$.

The unitary matrix $\mathbf{U}$ can also be found up to permutation and phase shifts by a combined JD/JOD of the two sets $\{\underline{\mathbf{D}}_{zz}(n_a,k_a)|a = 1,\ldots,P\}$ and $\{\underline{\mathbf{D}}_{zz}^c(n_c,k_c)|c = 1,\ldots,Q\}$.

Once the unitary matrix $\mathbf{U}$ is obtained from either the JD, JOD, or combined JD/JOD, an estimate of the mixing matrix $\mathbf{A}$ can be computed by the product $\mathbf{W}^\#\mathbf{U}$, where $\mathbf{W}$ is the whitening matrix (see Section 25.4.1.2). An estimate of the source signals $\mathbf{s}(n)$ can then be obtained by the product $\mathbf{A}^\#\mathbf{z}(n)$.

25.4.6.2 Separating More Sources Than Sensors

A challenging problem consists of the blind separation of more sources than sensors (i.e., $L > K$); this problem, also known as the underdetermined blind source separation problem, was pointed out for the first time in [102] while separating discrete sources. Since then, several other works based on *a priori* knowledge of the probability density functions of the sources [103, 104] were conducted. In [105], an approach for the resolution of the aforementioned problem exploits the concept of disjoint orthogonality of short Fourier transforms. Herein, for the resolution of the underdetermined problem, we review a STFD-based blind source separation method [84].

We start by selecting autoterm points where only one source exists, as described in Section 25.4.4. The corresponding STFD then has the following form:

$$\mathbf{D}_{\mathbf{zz}}(n,k) = D_{s_i s_i}(n,k)\mathbf{a}_i\mathbf{a}_i^H, \text{ where } (n,k) \in \Omega_i \tag{25.84}$$

where Ω_i denotes the time–frequency support of the ith source. The idea of the algorithm consists of clustering together the autoterm points associated with the same principal eigenvector of $\mathbf{D}_{\mathbf{zz}}(n,k)$ representing a particular source signal. Once the clustering and classification of the autoterms are done, the estimates of the source signals are obtained from the selected autoterms using a time–frequency synthesis algorithm [20]. Note that the missing autoterms in the classification, often due to intersection points, are automatically interpolated in the synthesis process. An advanced clustering technique of the above autoterms based on gap statistics is proposed in [106].

25.4.6.3 Separation of Convolutive Mixtures

Consider a convolutive multiple-input multiple-output linear time-invariant model given by

$$z_i(n) = \sum_{j=1}^{L}\sum_{c=0}^{C} a_{ij}(c)s_j(n-c) \text{ for } i = 1,\ldots,K \tag{25.85}$$

where $s_j(n)$, $j = 1,\ldots,L$, are the L source signals; $z_i(n)$, $i = 1,\ldots,K$, are the $K > L$ sensor signals; and $a_{ij}(c)$ is the transfer function between the jth source and the ith sensor with an overall extent of $(C+1)$ taps. The sources are assumed to have different time–frequency signatures, and the channel matrix $\mathbf{A}$ defined below in Equation 25.87 is full column rank.

In matrix form, Equation 25.85 becomes

$$\mathbf{z}(n) = \mathbf{A}\mathbf{s}(n) \tag{25.86}$$

where

$$\mathbf{s}(n) = [s_1(n),\ldots,s_1(n-(C+C')+1),\ldots,s_L(n-(C+C')+1)]^T$$
$$\mathbf{z}(n) = [z_1(n),\ldots,z_1(n-C'+1),\ldots,z_K(n-C'+1)]^T$$

$$\mathbf{A} = \begin{bmatrix} \mathbf{A}_{11} & \cdots & \mathbf{A}_{1L} \\ \vdots & \ddots & \vdots \\ \mathbf{A}_{K1} & \cdots & \mathbf{A}_{KL} \end{bmatrix} \tag{25.87}$$

with

$$\mathbf{A}_{ij} = \begin{bmatrix} a_{ij}(0) & \cdots & a_{ij}(C) & \cdots & 0 \\ & \ddots & \ddots & \ddots & \\ 0 & \cdots & a_{ij}(0) & \cdots & a_{ij}(C) \end{bmatrix} \tag{25.88}$$

Note that $\mathbf{A}$ is a $[KC' \times L(C+C')]$ matrix and $\mathbf{A}_{ij}$ are $[C' \times (C+C')]$ matrices. C' is chosen such that $KC' \geq L(C+C')$.

Herein, the same formalism as in the instantaneous mixture case is retrieved and the data STFDs still have the same expression as in Equation 25.56. However, the source auto-STFDs, $\mathbf{D}_{\mathbf{ss}}^a(n,k)$, are not diagonal but block diagonal with diagonal blocks of size $(C+C') \times (C+C')$. Note that the block diagonal structure comes from the fact that the cross-terms between $s_i(n)$ and $s_i(n-d)$, where d is some delay, are not zero and depend on the local correlation structure of the signal. This block diagonal structure is exploited to achieve the separation of the convolutive mixture.

25.4.6.4 STFD-Based Separation

First the data vector $\mathbf{z}(n)$ is whitened. The whitening matrix $\mathbf{W}$ is of size $[L(C'+C) \times KC']$ and verifies

$$\mathbf{W}E\{\mathbf{z}(n)\mathbf{z}(n)^H\}\mathbf{W}^H = \mathbf{W}\mathbf{R}_{\mathbf{zz}}\mathbf{W}^H = (\mathbf{W}\mathbf{A}\mathbf{R}_{\mathbf{ss}}^{\frac{1}{2}})(\mathbf{W}\mathbf{A}\mathbf{R}_{\mathbf{ss}}^{\frac{1}{2}})^H = \mathbf{I} \tag{25.89}$$

where $\mathbf{R}_{\mathbf{zz}}$ and $\mathbf{R}_{\mathbf{ss}}$ denote the covariance matrices of $\mathbf{z}(n)$ and $\mathbf{s}(n)$, respectively. Equation 25.89 shows that if $\mathbf{W}$ is a whitening matrix, then

$$\mathbf{U} = \mathbf{W}\mathbf{A}\mathbf{R}_{\mathbf{ss}}^{\frac{1}{2}} \tag{25.90}$$

is a $L(C'+C) \times L(C'+C)$ unitary matrix where $\mathbf{R}_{\mathbf{ss}}^{\frac{1}{2}}$ (Hermitian square root matrix of $\mathbf{R}_{\mathbf{ss}}$) is block diagonal. The whitening matrix $\mathbf{W}$ can be determined from the eigendecomposition of the data covariance matrix $\mathbf{R}_{\mathbf{zz}}$ as in [78].

Now by considering the whitened STFD matrices $\underline{\mathbf{D}}_{\mathbf{zz}}(n,k)$ and the above relations, we obtain the key relation

$$\underline{\mathbf{D}}_{\mathbf{zz}}(n,k) = \mathbf{U}\mathbf{R}_{\mathbf{ss}}^{-\frac{1}{2}}\mathbf{D}_{\mathbf{ss}}(n,k)\mathbf{R}_{\mathbf{ss}}^{-\frac{1}{2}}\mathbf{U}^H = \mathbf{U}\mathbf{D}(n,k)\mathbf{U}^H \tag{25.91}$$

where $\mathbf{D}(n,k) = \mathbf{R}_{\mathbf{ss}}^{-\frac{1}{2}}\mathbf{D}_{\mathbf{ss}}(n,k)\mathbf{R}_{\mathbf{ss}}^{-\frac{1}{2}}$.

Since the matrix $\mathbf{U}$ is unitary and $\mathbf{D}(n,k)$ is block diagonal, the latter just means that any whitened STFD matrix is block diagonal in the basis of the column vectors of matrix $\mathbf{U}$. The unitary matrix can be retrieved by computing the block diagonalization of some matrix $\underline{\mathbf{D}}_{\mathbf{zz}}(n,k)$. But to reduce the likelihood of indeterminacy and increase the robustness of determining $\mathbf{U}$, we consider the JBD of a set $\{\underline{\mathbf{D}}_{\mathbf{zz}}(n_l,k_l);\ l = 1,\ldots,P\}$ of P whitened STFD matrices. This JBD is achieved by the maximization under unitary transform of the following criterion:

$$C(\mathbf{U}) \triangleq \sum_{l=1}^{P}\sum_{m=1}^{L}\sum_{i,j=(C'+C)(m-1)+1}^{(C'+C)m} \left|\mathbf{u}_i^H\underline{\mathbf{D}}_{\mathbf{zz}}(n_l,k_l)\mathbf{u}_j\right|^2 \tag{25.92}$$

over the set of unitary matrices $\mathbf{U} = [\mathbf{u}_1,\ldots,\mathbf{u}_{L(C'+C)}]$. Note that an efficient Jacobi-like algorithm for the minimization of Equation 25.92 exists in [98, 107].

Once the unitary matrix $\mathbf{U}$ is determined up to a block diagonal unitary matrix $\mathbf{D}$ coming from the inherent indeterminacy of the JBD problem [108], the recovered signals are obtained up to a filter by

$$\hat{\mathbf{s}}(n) = \mathbf{U}^H\mathbf{W}\mathbf{z}(n) \tag{25.93}$$

According to Equations 25.86 and 25.90, the recovered signals verify

$$\hat{\mathbf{s}}(n) = \tilde{\mathbf{D}}\mathbf{s}(n) \tag{25.94}$$

with

$$\tilde{\mathbf{D}} = \mathbf{D}\mathbf{R}_{\mathbf{ss}}^{-\frac{1}{2}} \tag{25.95}$$

where we recall that the matrix $\mathbf{R}_{\mathbf{ss}}^{-\frac{1}{2}}$ and $\mathbf{D}$ are the block diagonal matrix and unitary block diagonal matrix, respectively. Consequently, $\tilde{\mathbf{D}}$ is also a block diagonal matrix, and the above STFD-based technique leads to the separation of the convolutive mixture up to a filter instead of a full MIMO deconvolution procedure.

Note that if needed, a SIMO (single-input multi-output) deconvolution/equalization [109] can be applied to the estimated sources of Equation 25.94.

25.5 Other TFSP Applications in Wireless Communications

25.5.1 Precoding for LTV Channels

Linear precoding is a useful signal processing tool for coping with frequency-selective propagation channels encountered with high-rate wireless transmission.

Precoding consists of mapping each incoming block of M symbols onto a P-long vector through a $P \times M$ ($P > M$) matrix referred to as the precoding matrix. Each received block is then multiplied by a $M \times P$ decoding matrix to retrieve the original symbols under the condition $M > L$ and $P = M + L$, where L is the overall channel length. To avoid interblock interference, guard intervals can be used, as in OFDM, for example. This can be done by forcing either the last L rows of the precoding matrix or the first L columns of the decoding matrix to zero [110].

Precoding of LTV channels can be optimized by *a priori* knowledge of the channel temporal evolution. This knowledge can be provided by a feedback channel such that the receiver estimates periodically the channel parameters, also called channel status information (CSI) [110], and sends them back to the transmitter. The latter uses this CSI to predict the channel evolution within a finite time interval and commutes the optimal precoder. The optimality herein should be understood in the sense of maximizing the information rate over the linear channel affected by additive Gaussian noise. Under the constraint of a fixed average transmit power, the optimal precoder, i.e., the optimal precoding matrix, is obtained from the SVD of the channel matrix[15] [111, 113].

In [110], a physical interpretation of the optimal precoding for time- and frequency-dispersive channels is provided thanks to an approximate analytic model for the eigenfunctions of LTV channels.[16] The approximate model is valid for multipath channels with finite Doppler and delay spread. Under the above model and using a time–frequency representation of the eigenfunctions, the latter are shown to be characterized by an energy distribution along curves, in the time–frequency plane, given by contour lines of the time–frequency representation of the LTV channel. In the same reference, it is also shown under mild conditions often met in practice that the TFDs of the right singular vectors of the LTV channel are mainly concentrated along the curves where the energy in the time–frequency domain of the channel equals the square of the associated singular value. The TFDs of the left singular vectors are simply time- and frequency-shift versions of the TFDs of the right singular vectors. This interpretation clearly establishes the optimal power allocation in the time–frequency domain as a generalization of the well-known water-filling principle [112, 114]. The above interpretation also allows an approximate computation of the channel singular vectors and values directly from the time–frequency representation of the LTV channel, without computing the SVD.

25.5.2 Signaling Using Chirp Modulation

TFSP tools can be used for the receiver design and for optimizing the design parameters of a spreading system using a chirp modulation scheme.

Indeed, chirp signals or, equivalently, linear FM signals have been widely used in sonar applications for range and Doppler estimation, as well as in radar systems for pulse compression. Thanks to their particular time–frequency signatures, these signals provide high interference rejection and inherent immunity against

[15]The channel matrix is the transfer matrix from the transmitted block vector to the received block vector.

[16]$v(t)$ is said to be an eigenfunction of $f(t)$ if and only if $\lambda v(t) = \int_{-\infty}^{+\infty} f(t-t')v(t')dt'$, where λ is known as the associated eigenvalue.

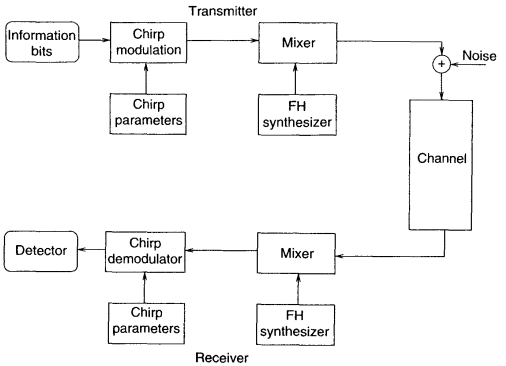

FIGURE 25.11 Chirp modulation signaling and FH communications system.

Doppler shift and multipath fading [115] in wireless communications. In addition, they are bandwidth efficient [117]. It have been shown [118] that for a same SNR and Doppler shift, the chirp signaling outperforms the frequency shift keying (FSK) signaling, thanks to their better cross-coherence properties, compared to FSK.

Signaling using chirp modulation is also seen as a spread-spectrum technique, which is defined as "a mean of transmission in which the signal occupies a bandwidth in excess of the minimum necessary to send the information" [41]. Chirp modulation was first suggested in [117] by using a pair of linear chirps with opposite chirp rates for binary signaling. A system for multiple access within a common frequency band was proposed in [119] by assigning pairs of linear chirps with different chirp rates to several users. In this system, the number of users simultaneously accessing the shared resources is limited by the MAI for a given time–bandwidth product. To reduce this shortcoming, the chirp signals are selected in [116] such that they all have the same power as well as the same bandwidth, offering inherent protection against frequency-selective fading. Further, the combination of chirp modulation signaling with frequency-hopping (FH) multiple access was proposed in [115]. The obtained hybrid system (Figure 25.11) improves communications system performance, especially in multipath fading-dispersive channels. Note that this system was extended to FH-CDMA in [120] and compared to the FSK-FH-CDMA system, leading to the same conclusion as in [115]. In [121], the chirp parameters, to be used in chirp modulation signaling, are selected under the actual time–bandwidth requirements so as to reduce significantly multiple-access interference and bit error rates.

25.5.3 Detection of FM Signals in Rayleigh Fading

Diversity reception is currently one of the most effective techniques for coping with the multipath Rayleigh fading effect in mobile environments [5]. It requires a number of signal transmission paths that carry the same information but have uncorrelated multipath fadings. A circuit to combine the received signals or select one of the paths is necessary. Diversity techniques take advantage of the fact that signals exhibit fades at different places in time, frequency, or space, depending on different situations. However, a diversity scheme normally requires a number of antennae at the transmitter or receiver, resulting in high cost and redundancy of information. Herein, we review a method that can overcome this problem.

Given a transmitted signal $s(t)$ under such an environment, the received signal $\underline{x}(t)$[17] is then considered random and may be modeled as [5]

$$\underline{x}(t) = \sum_{i=1}^{N} \underline{a}_i s(t - \underline{\tau}_i) \exp\{j\underline{\theta}_i\} \tag{25.96}$$

where N is the number of received waves and $\underline{a}_i$, $\underline{\tau}_i$, and $\underline{\theta}_i$ are the random attenuation, multipath delay, and phase shift associated with the ith path, respectively. When considering narrowband communications with frequency or phase modulation, the transmitted signals have the following form:

$$s(t) = \exp\{j[2\pi f_o t + \Psi_s(t)]\} \tag{25.97}$$

where $\Psi_s(t)$ represents the baseband signal and f_o is the carrier frequency. The received signal $\underline{x}(t)$ will then be expressed as

$$\underline{x}(t) = \underline{r}(t) \exp\{j[2\pi f_o t + \Psi_s(t) + \underline{\Psi}_r(t)]\} \tag{25.98}$$

For non-Rician channels (in general, channels with no line-of-sight path), envelope $\underline{r}(t)$ can be assumed to be Rayleigh distributed and hence has an autocorrelation function approximated by [122]

$$R_r(\tau) \approx \alpha(1 + 1/4\eta(\tau)) \tag{25.99}$$

where α is some constant and $\eta(\tau)$ is some particular function. The Fourier transform of the latter, referred to as S_η, exhibits a peak at the zero frequency [5]. The spectrum of the signal envelope is then given by

$$S_R(f) = \alpha(\delta(f) + \frac{1}{4}S_\eta(f)) \tag{25.100}$$

In [124, 125], it is shown that for various types of frequency modulation, the second-order Wigner–Ville spectrum (WVS)[18] (or spectra of other TFDs) of the received FM signal $\underline{x}(t)$ has a delta concentration along the IF of the transmitted signal. The special structure of the envelope spectrum (Equation 25.100) makes the delta concentration possible in the TF plane of the WVS (or spectra of other TFDs). Consequently, the detection of FM signals through the Rayleigh flat fading environment can be achieved in the above time–frequency plane without the use of the conventional diversity techniques or higher-order spectra approach [126].

25.5.4 Mobile Velocity/Doppler Estimation Using Time–Frequency Processing

Many wireless communications systems require prior knowledge of the mobile velocity. This knowledge allows compensation of distortions introduced by the communications channel. In addition, reliable estimates of the mobile velocity are useful for effective dynamic channel assignment and for the optimization of adaptive multiple access. In another chapter of [127], an overview of existing velocity estimators is given, particularly an estimator based on the estimation of the IF of the received signal. In contrast to approaches based on the envelope of the received signal, the IF-based velocity estimators are robust to shadow fading, which is produced by variations of the average of the received signal envelope over few wavelengths. Interested readers can refer to [127] for more details.

[17] Random terms are hereafter underlined to distinguish them from deterministic terms.

[18] The second-order time-varying Wigner–Ville spectrum is defined as [123]

$$\mathcal{W}^{(2)}_{\underline{x}}(t, f) \triangleq \int_{-\infty}^{\infty} E\{\underline{x}(t + \tau/2)\underline{x}^*(t - \tau/2)\}e^{-j2\pi f\tau} d\tau$$

25.6 Conclusion

The review of contributions made in applying TFSP to communications in general and wireless communications in particular indicates a wide range of possible uses of TFSP methods and techniques in these areas. Introducing the basics of TFSP and the motivation behind the use of TFSP techniques in wireless communications allowed the obtaining of a deeper understanding of how to match the properties of TFSP to the problems encountered in wireless communications. The application of TFSP in spread-spectrum communications systems includes channel identification, scattering function estimation, and interference (MAI and ISI) mitigation. Improvements of performance can be obtained in all these areas by adapting TFSP methodologies. Similarly, time–frequency array processing techniques are well suited for source localization and blind source separation. Other application issues in wireless communications that we are briefly discussed show that there are great potential benefits in further exploring the use of TFSP techniques for current issues in wireless communications and, more generally, in telecommunications.

In particular, note that the use of TFSP in spread-spectrum and array processing applications attracts more and more attention within the signal processing and communications communities. Indeed, using spatial diversity in conjunction with time and frequency diversity is a very powerful means of exploiting and extracting the received signal information. This is the main motivation behind the increasing number of TFSP-based array processing methods and applications that include source localization and source separation problems.

On the other hand, the spread-spectrum-based applications are driven by the fact that the third and most probably the fourth mobile generation systems will be based on the CDMA/MC-CDMA transmission technique. In such systems, the need to combat interuser interference and interchannel interference leads to the problem of the design of an orthogonal function in the time–frequency domain. Past and present research work has been and is being conducted to optimize the modulation/transmission scheme (e.g., by using chirp modulation) as well as the receiver/detection scheme. However, no final or optimal solution is available yet, and many open problems are still to be solved, for example, by using TFSP theories and methods.

Acknowledgments

The first author acknowledges the funding received from the Australian Research Council. The authors also acknowledge the assistance provided by G. Azemi, A.M. Khalighi, and S.A.C. Alvarez in the review of this chapter.

References

[1] H.V. Poor and G.W. Wornell, Eds., *Wireless Communications: Signal Processing Perspectives*, Englewood Cliffs, NJ: Prentice Hall, 1998.

[2] B. Boashash, Ed., *Time-Frequency Signal Analysis, Methods and Applications*, Melbourne, Australia: Longman Cheshire, 1992.

[3] B. Boashash, *Time-Frequency Signal Analysis and Processing: A Comprehensive Reference*, Oxford: Elsevier, 2003.

[4] L. Cohen, *Time-Frequency Analysis*, Englewood Cliffs, NJ: Prentice Hall, 1995.

[5] W. Jakes, Ed., *Microwave Mobile Communications*, Washington, DC: IEEE Press, 1998 (reprint).

[6] T.S. Rappaport, *Wireless Communications: Principles and Practice*, Englewood Cliffs, NJ: Prentice Hall, 1996.

[7] N. Martins, S. Jesus, C. Gervaise, and A. Quinquis, "A time-frequency approach to blind deconvolution in multipath underwater channels," in *Proceedings of IEEE International Conference on Acoustics, Speech, and Signal Processing (ICASSP)*, Vol. 2, 2002, pp. 1225–1228.

[8] X. Wang and J. Ray Liu, "Channel estimation for multicarrier modulation systems using a time-frequency polynomial model," *IEEE Transactions on Communications*, 50, 1045–1048, 2002.
[9] P. Bello, "Characterization of randomly time-variant linear channels," *IEEE Transactions on Communication Systems*, COM-11, 360–393, 1963.
[10] J.D.D. Parsons and A.S. Bajwa, "Wideband characterisation of fading mobile radio channels," *IEE Proceedings. F. Communications, Radar and Signal Processing*, 129, 95–101, 1982.
[11] K. Pahlavan and A. Levesque, *Wireless Information Networks*, New York: Wiley Interscience, 1995.
[12] R. Steele and L. Hanzo, Eds., *Mobile Radio Communications: Second and Third Generation Cellular and WATM Systems*, 2nd ed., Oxford: John Wiley & Sons, 1999.
[13] J.G. Proakis, *Digital Communications*, 4th ed., New York, McGraw-Hill, 2001.
[14] F. Swarts, P. van Rooyan, I. Oppermann, and M.P. Lotter, Eds., *CDMA Techniques for Third Generation Mobile Systems*, Boston: Kluwer Academic Publishers, 1999.
[15] R. Becher, M. Dillinger, M. Haardt, and W. Mohr, "Broad-band wireless access and future communication networks," *Proceedings of the IEEE*, 89, 58–75, 2001.
[16] L.B. Milstein, "Interference rejection techniques in spread spectrum communications," *Proceedings of the IEEE*, 657–671, 1988.
[17] S. Verdú, *Multiuser Detection*, Cambridge, U.K.: Cambridge University Press, 1998.
[18] V. Sucic, B. Barkat, and B. Boashash, "Performance evaluation of the B distribution," in *Proceedings of the Fifth International Symposium on Signal Processing and Its Applications, ISSPA '99*, Vol. 1, Brisbane, Queensland, Australia, August 1999, pp. 267–270.
[19] B. Boashash and V. Sucic, "Resolution measure criteria for the objective assessment of the performance of quadratic time–frequency distributions," *IEEE Transactions on Signal Processing*, 51, 1253–1263, 2003.
[20] G.F. Boudreaux-Bartels and T.W. Marks, "Time-varying filtering and signal estimation using Wigner distributions," *IEEE Transactions on Acoustics, Speech, and Signal Processing*, 34, 422–430, 1986.
[21] B. Boashash, "Time-frequency signal analysis," in *Advances in Spectrum Analysis and Array Processing*, Vol. I, S. Haykin, Ed., Englewood Cliffs, NJ: Prentice Hall, 1991, chap. 9, pp. 418–517.
[22] T.J. McHale and G.F. Boudreaux-Bartels, "An algorithm for synthesizing signals from partial time-frequency models using the cross Wigner distribution," *IEEE Transactions on Signal Processing*, 41, 1986–1990, 1993.
[23] J.C. Wood and D.T. Barry, "Linear signal synthesis using the Radon-Wigner transform," *IEEE Transactions on Signal Processing*, 42, 2105–2111, 1994.
[24] F. Hlawatsch and W. Krattenthaler, "Signal synthesis algorithms for bilinear time-frequency signal representations," in *The Wigner Distribution: Theory and Applications in Signal Processing*, W. Mecklenbräuker and F. Hlawatsch, Eds., Amsterdam: Elsevier, 1997, pp. 135–209.
[25] A. Francos and M. Porat, "Analysis and synthesis of multicomponent signals using positive time-frequency distributions," *IEEE Transactions on Signal Processing*, 47, 493–504, 1999.
[26] A.M. Sayeed, A. Sendonaris, and B. Aazhang, "Multiuser detection in fast-fading multipath environments," *IEEE Journal on Selected Areas in Communications*, 16, 1691–1701, 1998.
[27] H. Artés and F. Hlawatsch, "Blind multiuser equalization for time-varying channels," in *IEEE Signal Processing Workshop on Signal Proceeding Advances in Wireless Communications, SPAWC'01*, Taoyuan, Taiwan, March 2001, pp. 102–105.
[28] A.M. Sayeed and B. Aazhang, "Exploiting Doppler diversity in mobile wireless communications," in *Proceedings of CISS '97, 1997 Conference on Information Science Systems*, 1997, pp. 287–292.
[29] M.R. Baissas and A.M. Sayeed, "Pilot-based estimation of time-varying multipath channels for CDMA systems," in *International Conference on Acoustics, Speech, and Signal Processing, ICASSP '2000*, Vol. V, Istanbul, Turkey, June 2000, pp. 2657–2660.
[30] M.R. Baissas and A.M. Sayeed, "Channel estimation errors versus Doppler diversity in fast fading channels," in *Proceedings of the Thirty-Fourth Asilomar Conference*, Vol. 2, 2000, pp. 970–974.
[31] N.T. Gaarder, "Scattering function estimation," *IEEE Transactions on Information Theory*, IT-14, 684–693, 1968.

[32] H.L. VanTrees, *Detection, Estimation, and Modulation Theory. Radar-Sonar Signal Processing and Gaussian Signals in Noise*, Malabar, FL, Krieger Publication Co., 1992.
[33] R.A. Altes, "Detection, estimation, and classification with spectrograms," *The Journal of the Acoustical Society of America*, 67, 1232–1246, 1980.
[34] P. Flandrin, "A time-frequency formulation of optimum detection," *IEEE Transactions on Acoustics, Speech, and Signal Processing*, 36, 1377–1384, 1988.
[35] B.L. Johnson, D.W. Ricker, and J.R. Sacha, "The use of iterative deconvolution for scattering function identification," *The Journal of the Acoustical Society of America*, 91, 2790–2798, 1992.
[36] D.W. Ricker and M.J. Gustafson, "A low sidelobe technique for the direct measurement of scattering functions," *IEEE Journal of Oceanic Engineering*, 21, 14–23, 1996.
[37] T. Wang, V.K. Dubey, and J.T. Ong, "Generation of scattering functions for mobile communication channel: a computer simulation approach," *Wireless Information Networks*, 4, 187–204, 1997.
[38] J.S. Sadowsky and V. Kafedziski, "On the correlation and scattering function of the WSSUS channel for mobile communications," *IEEE Transactions on Vehicular Technology*, 47, 270–282, 1998.
[39] L.-T. Nguyen, B. Senadji, and B. Boashash, "Scattering function and time-frequency signal processing," in *International Conference on Acoustics, Speech, and Signal Processing, ICASSP 2001*, Salt Lake City, UT, June 2001.
[40] R. Haas and J.-C. Belfiore, "A time-frequency well-localized pulse for multiple carrier transmission," *Wireless Personal Communications*, 5, 1–18, 1997.
[41] R.L. Pickholtz, L.B. Milstein, and D.L. Schilling, "Spread spectrum for mobile communications," *IEEE Transactions on Vehicular Technology*, 40, 313–322, 1991.
[42] E. Marsy, "Closed-form analytical results for the rejection of narrowband interference in PN spread spectrum systems. Part I. Linear prediction filters," *IEEE Transactions on Communications*, COM–32, 888–896, 1984.
[43] H.V. Poor and L.A. Rusch, "Narrowband interference suppression in spread spectrum CDMA," *IEEE Personal Communications*, Third Quarter, 14–27, 1994.
[44] L.A. Rusch and H.V. Poor, "Multiuser detection techniques for narrowband interference suppression in spread spectrum communications," *IEEE Transactions on Communications*, 43, 1725–1737, 1995.
[45] H.V. Poor and X. Wang, "Blind adaptive suppression of narrowband digital interferers from spread spectrum signals," *Wireless Personal Communications*, 6, 69–96, 1998.
[46] A. Bultan and A.N. Akansu, "A novel time-frequency exciser in spread spectrum communications for chirp-like interference," in *International Conference on Acoustics, Speech, and Signal Processing, ICASSP '98*, Vol. 6, 1998, pp. 3265–3268.
[47] A. Bultan, M.V. Tazebay, and A.N. Akansu, "A comparative performance study of excisers for various interference classes," in *Proceedings of the IEEE-SP International Symposium on Time-Frequency and Time-Scale Analysis*, New York, 1998, pp. 381–384.
[48] S.-H. Hong and B.G. Lee, "Time-frequency localized subspace tracking for narrowband interference suppression of DS/CDMA systems," *Electronics Letters*, 35, 1063–1064, 1999.
[49] J. Horng and R.A. Haddad, "Interference excision in DSSS communication system using time-frequency adaptive block transform," in *Proceedings of the IEEE-SP International Symposium on Time-Frequency and Time-Scale Analysis*, Pittsburgh, PA, October 6–9, 1998, pp. 385–388.
[50] M.V. Tazebay and A.N. Akansu, "Adaptive subband transforms in time-frequency excisers for DSSS communications systems," *IEEE Transactions on Signal Processing*, 43, 2776–2782, 1995.
[51] M.V. Tazebay and A.N. Akansu, "A smart time-frequency exciser for spread spectrum communications," in *International Conference on Acoustics, Speech, and Signal Processing, ICASSP '95*, Vol. 2, New York, 1995, pp. 1209–1212.
[52] M.V. Tazebay and A.N. Akansu, "A performance analysis of interference excision techniques in direct sequence spread spectrum communications," *IEEE Transactions on Signal Processing*, 46, 2530–2535, 1998.

[53] B. Boashash, "Estimating and interpreting the instantaneous frequency of a signal. Part 2. Algorithms and applications," *Proceedings of the IEEE*, 80, 539–569, 1992.
[54] F. Hlawatsch and G.F. Boudreaux-Bartels, "Linear and quadratic time-frequency signal representations," *IEEE Signal Processing Magazine*, 9, 21–67, 1992.
[55] M.G. Amin, "Interference mitigation in spread spectrum communication systems using time-frequency distributions," *IEEE Transactions on Signal Processing*, 45, 90–101, 1997.
[56] M.G. Amin, C. Wang, and A.R. Lindsey, "Optimum interference excision in spread spectrum communications using open-loop adaptive filters," *IEEE Transactions on Signal Processing*, 47, 1966–1976, 1999.
[57] S. Barbarossa and A. Scaglione, "Adaptive time-varying cancellation of wideband interferences in spread-spectrum communications based on time-frequency distributions," *IEEE Transactions on Signal Processing*, 47, 957–965, 1999.
[58] S. Barbarossa, A. Scaglione, S. Spalletta, and S. Votini, "Adaptive suppression of wideband interferences in spread-spectrum communications using the Wigner-Hough transform," in *International Conference on Acoustics, Speech, and Signal Processing, ICASSP '97*, Vol. 5, California, 1997, pp. 3861–3864.
[59] S. Lach, M.G. Amin, and A. Lindsey, "Broadband interference excision for software-radio spread-spectrum communications using time-frequency distribution synthesis," *IEEE Journal on Selected Areas in Communications*, 17, 704–714, 1999.
[60] X. Ouyang and M.G. Amin, "Performance analysis of the DS/SS communications receiver implementing a short time Fourier transform interference excision system," in *Proceedings of the IEEE-SP International Symposium on Time-Frequency and Time-Scale Analysis*, Pittsburgh, PA, October 6–9, 1998, pp. 393–396.
[61] X. Ouyang and M.G. Amin, "Short-time Fourier transform receiver for nonstationary interference excision in direct sequence spread spectrum communications," *IEEE Transactions on Signal Processing*, 49, 851–863, 2001.
[62] S. Barbarossa, "Analysis of multicomponent LFM signals by a combined Wigner-Hough transform," *IEEE Transactions on Signal Processing*, 43, 1511–1515, 1995.
[63] B. Boashash and P. O'Shea, "Use of the cross Wigner-Ville distribution for estimation of instantaneous frequency," *IEEE Transactions on Signal Processing*, 41, 1439–1445, 1993.
[64] R. Prasad, *CDMA for Wireless Personal Communications*, Mobile Communications Series, Artech House, Norwood, MA, 1997.
[65] K. Fazel, "Performance of CDMA/OFDM for mobile communication systems," in *Proceedings of the IEEE 2th ICUPC*, Ottawa, Canada, 1993, pp. 975–979.
[66] S. Hara and R. Prasad, "Overview of multicarrier CDMA," *IEEE Communications Magazine*, 35, 126–133, 1997.
[67] S. Hara and R. Prasad, "Design and performance of multicarrier CDMA system in frequency-selective Rayleigh fading channels," *IEEE Transactions on Vehicular Technology*, 48, 1584–1595, 1999.
[68] N. Yee, J.-P. Linnartz, and G.P. Fettweis, "Multi-carrier CDMA in indoor wireless radio networks," in *Proceedings of the IEEE 4th PIMRC*, Yokohama, Japan, 1993, pp. 109–113.
[69] K.D. Kammeyer, U. Tuisel, H. Schulze, and H. Bochmann, "Digital multicarrier: transmission of audio signals over mobile radio channels," *European Transactions on Telecommunications*, 3, 243–253, 1992.
[70] R.W. Chang, "Synthesis of band-limited orthogonal signals for multichannel data transmission," *Bell System Technical Journal*, 45, 1775–1796, 1966.
[71] J. Kühne, A. Nahler, and G.P. Fettweis, "Multi-user interference evaluation for a one-code multi-carrier spread spectrum CDMA system with imperfect time and frequency synchronization," in *1988 IEEE 5th International Symposium on Spread Spectrum Techniques and Applications — Proceedings. Spread Technology to Africa*, Vol. 2, New York, 1998, pp. 479–483.
[72] V. Aue and G.P. Fettweis, "Multi-carrier spread spectrum modulation with reduced dynamic range," in *Proceedings of the 46th IEEE Vehicular Technology Conference*, April 1996, pp. 914–917.

[73] S. Verdu, *Multiuser Detection*, New York: Cambridge University Press, 1998.
[74] A.H. Sayed and N.R. Yousef, "Wireless location", in *Wiley Encyclopedia of Telecommunications*, J. Proakis, Ed., New York: Wiley & Sons, 2002.
[75] A. Belouchrani and M.G. Amin, "A new approach for blind source separation using time frequency distributions," in *Proceedings SPIE Conference on Advanced Algorithms and Architectures for Signal Processing*, Denver, Colorado, August 1996.
[76] A. Belouchrani and M.G. Amin, "Blind source separation using time-frequency distributions: algorithm and asymptotic performance," in *IEEE Proceeding ICASSP*, Germany, April 1997.
[77] A. Belouchrani and M.G. Amin, "On the Use of Spatial Time Frequency Distributions for Signal Extraction," Special issue of the journal *Multidimensional Systems and Signal Processing*, Boston: Kluwer Academic Publishers, October 1998.
[78] A. Belouchrani and M.G. Amin, "Blind source separation based on time-frequency signal representation," *IEEE Transactions on Signal Proceedings*, 2888–2898, 1998.
[79] A. Belouchrani and M.G. Amin, "Time-frequency MUSIC: a new array signal processing method based on time-frequency signal representation," *IEEE Signal Processing Letters*, 6, 109–110, 1999.
[80] A.S. Kayhan and M.G. Amin, "Spatial evolutionary spectrum for DOA estimation and blind signal separation," *IEEE Transactions on Signal Processing*, 2000.
[81] A.R. Leyman, Z.M. Kamran, and K. Abed-Meraim, "Higher order time frequency based blind source separation technique," *IEEE Signal Processing Letters*, 2000.
[82] Y. Zhang, W. Mu, and M.G. Amin, "Subspace analysis of spatial time frequency distribution matrices," *IEEE Transactions on Signal Processing*, 49, 2001.
[83] A. Belouchrani, K. Abed-Meraim, M.G. Amin, and A. Zoubir, "Joint anti-diagonalization for blind source separation," in *Proceedings ICASSP*, Utah, Vol. 5, May 2001, pp. 2789–2792.
[84] L.-T. Nguyen, A. Belouchrani, K. Abed-Meraim, and B. Boashash, "Separating more sources than sensors using time frequency distributions," in *Proceeding ISSPA*, Kuala-Lampur, Malaysia, Vol. 2, August 2001, pp. 583–586.
[85] L. Giulieri, N. Thirion-Moreau, and P.-Y. Arques, "Blind sources separation based on bilinear time-frequency representations: a performance analysis," in *Proceedings ICASSP*, Vol. 2, 2002, pp. 1649–1652.
[86] L. Jin, Q.-Y. In, and W.-J. Wang, "Time-frequency signal subspace fitting method for direction-of-arrival estimation" in *Proceedings IEEE International Symposium on Circuits and Systems*, ISCAS '2000, Vol. 3, Geneva, May 2000, pp. 375–378.
[87] G. Wang and X.-G. Xia, "Iterative algorithm for direction of arrival estimation with wideband chirp signals," *IEE Proceedings: Radar, Sonar and Navigation*, 147, 233–238, 2000.
[88] L. Cirillo, A. Zoubir, N. Ma, and M.G. Amin, "Automatic classification of auto- and cross-terms of time-frequency distributions in antenna arrays," in *Proceedings of ICASSP*, Orlando, FL, 2002.
[89] A. Hassanien, A.B. Gershman, and M.G. Amin, "Time-frequency ESPRIT for direction-of-arrival estimation of chirp signals," in *Sensor Array and Multichannel Signal Processing Workshop Proceedings*, August 4–6, 2002, pp. 337–341.
[90] Y. Zhang and M.G. Amin, "Blind separation of sources based on their time-frequency signatures," in *Proceedings ICASSP*, Istanbul, Turkey, June 2000.
[91] M. Wax and T. Kailath, "Detection of signals by information theoretic criteria," *IEEE Transactions on Acoustic, Speech and Signal Processing*, ASSP-33, 387–392, 1985.
[92] L. Cirillo, A. Zoubir, and M.G. Amin, "Selection of auto- and cross-terms for blind non-stationary source separation," in *Proceedings of the IEEE International Symposium on Signal Processing and Information Technology (ISSPIT)*, Cairo, Egypt, 2001.
[93] W. Mu, M.G. Amin, and Y. Zhang, "Bilinear signal synthesis in array processing," *IEEE Transactions on Signal Processing*, 51, 90–100, 2003.
[94] L. Giulieri, N. Thirion-Moreau, and P.-Y. Arques, "Blind sources separation using bilinear and quadratic time-frequency representations," in *ICA '2001*, San Diego, December 2001.

[95] R. Schmidt, "Multiple emitter location and signal parameter estimation," *IEEE Transactions on Antennas and Propagation*, 34, 276–280, 1986.
[96] R. Roy and T. Kailath, "ESPRIT: estimation of signal parameters via rotational invariance techniques," *IEEE Transactions Acoustic, Speech, Signal Processing*, 37, 984–995, 1989.
[97] Y. Zhang, W. Mu, and M.G. Amin, "Time-frequency maximum likelihood methods for direction finding," *Journal Franklin Institue*, 337, 483–497, 2000.
[98] A. Belouchrani, M.G. Amin, and K. Abed-Meraim, "Direction finding in correlated noise fields based on joint block-diagonalization of spatio-temporal correlation matrices," *IEEE Signal Processing Letters*, 4, 266–268, 1997.
[99] A. Belouchrani, K. Abed-Meraim, J.F. Cardoso, and E. Moulines, "Blind source separation using second order statistics," *IEEE Transactions on Signal Proceedings*, 434–444, 1997.
[100] C. Jutten and J. Hérault, "Détection de grandeurs primitives dans un message composite par une architecture de calcul neuromimétrique en apprentissage non supervisé," in *Proceedings GRETSI*, Nice, France, 1985.
[101] P. Comon, "Independent component analysis, a new concept?" *Signal Processing*, 36, 287–314, 1994.
[102] A. Belouchrani and J.-F. Cardoso, "Maximum likelihood source separation for discrete sources," in *Proceedings EUSIPCO*, 1994, pp. 768–771.
[103] P. Comon and O. Grellier, "Nonlinear inversion of underdetermined mixtures," in *ICA '99*, Aussois, France, pp. 461–465, January 1999.
[104] K.I. Diamantaras, "Blind separation of multiple binary sources using a single linear mixture," in *International Conference on Acoustics, Speech, and Signal Processing, ICASSP '2000*, Istanbul, Turkey, Vol. V, June 2000, pp. 2657–2660.
[105] A. Jourjine, S. Rickard, and O. Yilmaz, "Blind separation of disjoint orthogonal signals: demixing *n* sources from 2 mixtures," in *International Conference on Acoustics, Speech, and Signal Processing, ICASSP '2000*, Istanbul, Turkey, Vol. 5, June 2000, pp. 2985–2988.
[106] Y. Luo and J. Chambers, "Active source selection using gap statistics for underdetermined blind source separation," in *Proceedings of the 7th International Symposium on Signal Processing and Its Applications (ISSPA)*, Vol. I, Paris, France, July 1–4, 2003, pp. 137–140.
[107] A. Belouchrani, K. Abed-Meraim, and Y. Hua, "Jacobi-like algorithms for joint block diagonalization: application to source localization," *in Proceedings ISPACS*, Melbourne, Australia, November 1998.
[108] H. Bousbia-Saleh, A. Belouchrani, and K. Abed-Meraim, "Jacobi-like algorithm for blind signal separation of convolutive mixtures," *Electronics Letters*, 37, 1049–1050, 2001.
[109] K. Abed-Meraim, W. Qiu, and Y. Hua, "Blind system identification," *Proceedings of the IEEE*, 85, 1310–1322, 1997.
[110] S. Barbarossa and A. Scaglione, "Optimal precoding for transmissions over linear time-varying channels," in *Proceedings of GLOBECOM '99*, Vol. 5, Piscataway, NJ, 1999, pp. 2545–2549.
[111] A. Scaglione, S. Barbarossa, and G.B. Giannakis, "Filterbank transceivers optimizing information rate in block transmissions over dispersive channels," *IEEE Transactions on Information Theory*, 45, 1019–1032, 1999.
[112] R.G. Gallager, *Information Theory and Reliable Communication*, New York: John Wiley & Sons, 1968.
[113] M. Medard, "The Capacity of Time-Varying Multiple User Channels in Wireless Communications," Ph.D. thesis, MIT, Cambridge, MA, September 1995.
[114] A. Goldsmith, "Design and Performance of High-Speed Communication Systems over Time-Varying Radio Channels," Ph.D. thesis, University of California, Berkeley, September 1994.
[115] S.E. El-Khamy, S.E. Shahban, and E.A. Thabet, "Frequency hopped multi-user chirp modulation (FH/MCM) for multipath fading channels," in *IEEE Symposium Antennas and Propagation*, Vol. 1, July 1999, pp. 996–999.
[116] S.E. El-Khamy, S.E. Shahban, and E.A. Thabet, "Efficient multiple access communications using multi-user chirp modulation signals," in *IEEE 4th International Symposium on Spread Spectrum Techniques and Applications*, Vol. 3, September 1996, pp. 1209–1213.

[117] M.R. Winkler, "Chirp Signals for Communications," WESCON convention record, Paper 14.2, 1962.
[118] A.J. Berni and W.D. Gregg, "On the utility of chirp modulation for digital signaling," *IEEE Transactions on Communications*, 1973.
[119] C.E. Cook, "Linear FM signal formats for beacon and communication systems," *IEEE Transactions on Aerospace and Electronic Systems*, 10, 471–478, 1974.
[120] C. Gupta and A. Papandreou-Suppappola, "Wireless CDMA communications using time-varying signals," in *Sixth International Symposium on Signal Processing and Its Applications*, Vol. 1, August 2001, pp. 242–245.
[121] S. Hengstler, D.P. Kasilingam, and A.H. Costa, "A novel chirp modulation spread spectrum technique for multiple access," in *IEEE Seventh International Symposium on Spread Spectrum Techniques and Applications*, Vol. 1, 2002, pp. 73–77.
[122] W.B. Davenport and W.L. Root, *An Introduction to the Theory of Random Signals and Noise*, Washington, DC: IEEE Press, 1987.
[123] B. Boashash and B. Ristic, "Polynomial time-frequency distributions and time-varying higher order spectra: application to the analysis of multicomponent FM signals and to the treatment of multiplicative noise," *Signal Processing*, 67, 1–23, 1998.
[124] L.-T. Nguyen and B. Senadji, "Analysis of nonlinear signals in the presence of Rayleigh fading," in *Proceedings of the Fifth International Symposium on Signal Processing and Its Applications, ISSPA '99*, Brisbane, Queensland, Australia, Vol. 1, August 1999, pp. 411–414.
[125] L.-T. Nguyen and B. Senadji, "Detection of frequency modulated signals in Rayleigh fading channels based on time-frequency distributions," in *International Conference on Acoustics, Speech, and Signal Processing, ICASSP '2000*, Vol. II, Istanbul, Turkey, June 2000, pp. 729–732.
[126] B. Senadji and B. Boashash, "A mobile communications application of time-varying higher order spectra to FM signals affected by multiplicative noise," in *Proceedings of ICICS, 1997 International Conference on Information, Communications, and Signal Processing*, Vol. 3, New York, 1997, pp. 1489–1492.
[127] B. Senadji, G. Azemi, and B. Boashash, "Mobile velocity estimation for wireless communications," chapter in *Signal Processing for Mobile Communications Handbook*, M. Ibnkahla, Ed., Boca Raton, FL: CRC Press, 2003.